

**EARLINET:  
A European Aerosol Research Lidar Network  
to Establish an Aerosol Climatology.**

**Contract EVR1-CT1999-40003**

**Scientific Report for the period  
February 2000 to January 2001.**

**March 28, 2001**

**Compiled by:**

**Jens Bösenberg  
Max-Planck-Institut für Meteorologie  
Bundesstr. 55  
D-20146 Hamburg**

# Contents

<b>1</b>	<b>Management report</b>	<b>5</b>
<b>2</b>	<b>Executive summary</b>	<b>6</b>
2.1	List of publications . . . . .	7
2.1.1	Peer reviewed articles: . . . . .	7
2.1.2	Non refereed literature: . . . . .	7
2.1.3	Others: . . . . .	7
<b>3</b>	<b>Progress of Work</b>	<b>8</b>
3.1	WP1, Hardware setup . . . . .	8
3.1.1	Objective . . . . .	8
3.1.2	Achievements . . . . .	8
3.1.3	Plans for the next period . . . . .	10
3.2	WP2, Regular measurements . . . . .	11
3.2.1	Objective . . . . .	11
3.2.2	Methodology . . . . .	11
3.2.3	Scientific Achievements . . . . .	11
3.2.4	Plan for the next period . . . . .	13
3.3	WP3, Quality assurance . . . . .	14
3.3.1	Algorithm intercomparison . . . . .	14
3.3.2	Instrument intercomparison . . . . .	18
3.4	WP4, Compilation of trajectory data . . . . .	26
3.4.1	Atmospheric trajectories for the EARLINET project . . . . .	26
3.4.2	Statistical analysis of trajectories . . . . .	26
3.4.3	First results of cluster analysis of trajectories . . . . .	28
3.4.4	Conclusions . . . . .	29
3.5	WP5, Compilation of aerosol profile data . . . . .	30
3.5.1	Objectives . . . . .	30
3.5.2	Methodology . . . . .	30
3.5.3	Scientific achievements . . . . .	30
3.5.4	Plans for the next period . . . . .	30
3.6	WP6, Temporal cycles . . . . .	31
3.6.1	Objectives . . . . .	31
3.6.2	Methodology and scientific achievements . . . . .	31
3.6.3	Socio-Economic relevance and policy implication . . . . .	33
3.6.4	Discussion and conclusion . . . . .	33
3.6.5	Plan and Objectives for the next period . . . . .	33

3.7	WP7, Observation of special events . . . . .	34
3.7.1	Objectives . . . . .	34
3.7.2	Methodology . . . . .	34
3.7.3	Scientific achievements . . . . .	34
3.7.4	Socio-economic relevance and policy implication . . . . .	37
3.7.5	Discussion and conclusion . . . . .	37
3.7.6	Plan and objectives for the next period . . . . .	38
3.8	WP8, Impact on satellite retrievals . . . . .	39
3.9	WP9, Air mass modification processes . . . . .	40
3.10	WP10, Orography and vertical transport . . . . .	42
3.10.1	Objectives . . . . .	42
3.10.2	Methods . . . . .	42
3.10.3	Scientific achievements . . . . .	42
3.10.4	Socio-economic relevance and policy implications . . . . .	42
3.10.5	Discussion and conclusion . . . . .	43
3.10.6	Plan and objectives for the next period . . . . .	43
3.11	WP11, Stratospheric aerosol . . . . .	44
3.12	WP12, Differences rural-urban aerosols . . . . .	45
3.12.1	Objectives . . . . .	45
3.12.2	Methodology and scientific achievements . . . . .	45
3.13	WP13, UV-B and optical properties . . . . .	46
3.13.1	Objectives . . . . .	46
3.13.2	Methodology and scientific achievements . . . . .	46
3.13.3	Discussion and conclusion . . . . .	46
3.13.4	Plan and objectives for the next period . . . . .	48
3.14	WP14, Statistical analysis . . . . .	49
3.15	WP15, Lidar ratio data base . . . . .	50
3.15.1	Objectives . . . . .	50
3.15.2	Methodology and scientific achievements . . . . .	50
3.15.3	Socio-economic relevance and policy implication . . . . .	50
3.15.4	Discussion and conclusion . . . . .	50
3.15.5	Plan and objectives for the next period . . . . .	51
3.16	WP16, Analysis of source regions . . . . .	52
3.16.1	Objectives . . . . .	52
3.16.2	Methods . . . . .	52
3.16.3	Scientific achievements . . . . .	52
3.16.4	Socio-economic relevance and policy implications . . . . .	52
3.16.5	Discussion and conclusion . . . . .	52
3.16.6	Plan and objectives for the next period . . . . .	53
3.17	WP17, Microphysical retrieval algorithms . . . . .	54
3.17.1	Objectives . . . . .	54
3.17.2	Methodology . . . . .	54
3.17.3	Scientific achievements . . . . .	55
3.17.4	Socio-Economic relevance and policy implication . . . . .	58
3.17.5	Discussion and conclusion . . . . .	58
3.17.6	Plan and Objectives for the next period . . . . .	59
3.18	General project assessment . . . . .	60

3.18.1	Objectives . . . . .	60
3.18.2	Scientific achievements . . . . .	60
3.18.3	Socio-economic relevance and policy implications . . . . .	60
3.18.4	Plan for the next period . . . . .	60

# Chapter 1

## Management report

See separate report, e.g. at <http://lidarb.dkrz.de/earlinet>

# Chapter 2

## Executive summary

### Objectives

The main objectives of EARLINET are the establishment of a comprehensive and quantitative statistical data base of the horizontal and vertical distribution of aerosols on the European scale using a network of advanced laser remote sensing stations, and the use of these data for studies related to the impact of aerosols on a variety of environmental problems. The main objectives for the reporting period were to get the network operation started, to establish common methodology, and to assure data quality.

### Scientific achievements

The first important step in the setup of the network was the preparation of the different lidar stations for the intended mode of operation. This was a major effort because only existing instruments are used which had been designed for different purposes. The task was successfully completed on schedule at almost all stations, with the only exceptions for stations where substantial reconstruction or upgrade works were necessary.

Great emphasis was put on the assurance of data quality. A comprehensive algorithm intercomparison was completed successfully after adjustment of some of the algorithms. It was decided to launch another intercomparison for the extinction retrievals, which is presently being performed. A rather big effort was made to compare the lidar systems directly in a series of experiments. Although a number of technical problems were detected for several systems, the campaign was very successful because the problems could be identified and either solved immediately or in the near future. Some intercomparisons are to be repeated, but the quality assessment will be completed on schedule.

The routine measurements for the establishment of a climatological data set have been conducted very well at most stations. For the first period of seven months a large data set of roughly 3000 individual profiles has been compiled and is available on CD-ROM. This is by far the largest data set on the vertical distribution of aerosol worldwide. The second long-term task, the compilation of trajectory data, was also started and continued on schedule. The data set of analytical backtrajectories for all stations will be used to identify source regions and important modification processes.

In addition to the routine measurements an extended special program has been performed addressing the observation of Saharan dust episodes mainly in the Mediterranean. It is considered a great success that a large data set has been collected on the vertical distribution of Saharan dust clouds, covering 13 episodes. Again this is the largest existing data set on that subject. It forms a solid basis for the investigation of associated atmospheric processes.

## **Socio-economic relevance and policy implications**

The main overall achievement of the first year is the formation and operation of a real network of 20 individual groups having very different starting positions. It is a major step forward that regular measurements with similar methods are performed at 20 stations on a truly continental scale, that equivalent retrieval methods are used, and that a growing data base is compiled which is used jointly by all partners. This is relevant with respect to the formation of a cooperative European scientific community in the area of advanced remote sensing and experimental environmental studies. Although the data set resulting from the project is still rather limited, it clearly is the best available instrument for studying issues related to the vertical distribution of aerosol. Worldwide there is no similar network, Europe has become the leader in this area of research and application of advanced measurement techniques. The studies on Saharan dust transport in the Mediterranean are of high importance for the assessment of the relative contributions from natural and anthropogenic sources to the overall aerosol load that can be very high particularly in these areas.

## **Conclusions**

The European Aerosol Research Lidar Network is established with good success. The methods that were selected or developed for the studies appear to be appropriate. The plan for the coming period is mainly to continue the regular and special measurements and to start with statistical analyses based on the growing data set.

## **2.1 List of publications**

### **2.1.1 Peer reviewed articles:**

Bösenberg, J., Ansmann, A., Baldasano, J., Balis, D., Böckmann, C., Calpini, B., Chaikovsky, A., Flamant, P., Hagard, A., Mitev, V., Papayannis, A., Pelon, J., Resendes, D., Schneider, J., Spinelli, N., Vaughan, T. T. G., Visconti, G., and Wiegner, M. (2000). EARLINET: A European Aerosol Research Lidar Network. In Dabas, A. and Pelon, J., editors, *Laser Remote Sensing of the Atmosphere. Selected Papers of the 20<sup>th</sup> International Laser Radar Conference*. Edition Ecole Polytechnique, Palaiseau, in press.

### **2.1.2 Non refereed literature:**

Schneider, J., Ansmann, A., Baldasano, J., Balis, D., Böckmann, C., Bösenberg, J., Calpini, B., Chaikovsky, A., Flamant, P., Hagard, A., Mitev, V., Papayannis, A., Pelon, J., Resendes, D., Spinelli, N., Vaughan, T. T. G., Visconti, G., and Wiegner, M. (2000). A European Aerosol Research Lidar Network to Establish an Aerosol Climatology: EARLINET. *J. Aerosol Science*, 31:592–593.

Böckmann, C. and Wauer, J. (2000). The influence of spheroids on the inversion in the retrieval of micro-physical particle parameters from lidar data. In *Proc. SPIE Intern. Soc. Opt. Eng. 4015, Sendai, Japan*.

Bösenberg, J. (ed.) (2000). EARLINET: Handbook of Instruments Internet publication on project page

### **2.1.3 Others:**

CD-ROM with aerosol data

CD-ROM with trajectory data

# Chapter 3

## Progress of Work

### Introduction

This chapter is organised strictly according to the structure of work packages as defined in the statement of work. No individual group reports are included. It is emphasized that all work package reports have been compiled using the input of a large number of individuals including all groups. It is considered a great advantage of this project that the work is performed in very close cooperation between many groups, with mutual benefits from the work of other partners. The disadvantage of course is that not always proper credit can be given to the individuals that have contributed. However, all these contributions are explicitly acknowledged here.

### 3.1 WP1, Hardware setup

by Jens Bösenberg

#### 3.1.1 Objective

The main goal of this work package was to prepare the lidar systems at all sites for proper operation within the network. The project is almost completely relying on existing hardware which is supplied by the individual partner institutions, only very few upgrades were supported through project money. The main challenge is the request for operation on a regular schedule, which is different from previous operation for most of the participants, but also the request for extended additional coordinated measurements. Considering the complexity of a lidar system the time for preparation of the instruments was extremely short. But in view of the main goal of the project, the compilation of a comprehensive climatological database of the aerosol vertical distribution, it was necessary to get started as early as possible, even if at some stations further improvements were still in progress.

#### 3.1.2 Achievements

At almost all stations the lidar systems were ready for operation as scheduled. The details of the used instruments are described in the handbook of instruments which has been published in September 2000 and which is available at <http://lidarb.dkrz.de/earlinet>. Table 3.1 provides an overview over the present and planned status of the hardware at the individual stations.



Station no.	ab	at	ba	gp	hh	ju	kb	la	lc	le	li	lk	mi	mi.2	mu	na	ne	pl	po	th
<b>Detection channels</b>																				
<b>elastic backscatter</b>																				
solar blind UV	x	u		x	u	x	x	x	x	x		x	x	u	x	x	x		x	x
UV		x		x	x	x	x				u		x	x				x		u
VIS		x	u	x	x	x	x						x	x				x		u
IR		x	x	x	x	x	x				x	u	x	x				x		u
<b>N<sub>2</sub> Raman scattering</b>																				
solar blind UV	x	u			u	x	x	x	x	x		u		u	x	x	u		x	u
UV					x		x													
VIS			u		x		x													
water vapor channel	x				u		u	x	u	x										
temperature channel							x													
depolarisation channel					u	x	x													
scanning capability			x	x					u		x	x	x	x	x					x
system transportable			x	x	x						x	x	x	x	x					x
altitude limit low	0.5	0.5	.25	0.2	0.3	4.0	1.0	0.3	0.4	0.3	0.3	0.1	0.1	0.5	0.2	.25	1.0	0.5	1.2	0.7
altitude limit high	8.0	5.0	10.	10.	9.0	11.	35.	12.	7.0	12.	5.0	10.	30.	10.	5.0	3.0	10.	15.	8.0	8.0
range resolution (raw)	30	7.5	7.5	15	15	7.5	50	300	15	60	1.5	7.5	15	15	3.75	15	30	15	15	7.5
time resolution (raw)	330	360	1800	10	10	100	33	300	180	30	1	.1	10	200	0.1	60	200	10	60	240

Table 3.1: Overview over main system characteristics. x = existing, u = planned upgrade

ab	Aberystwyth	at	Athens	ba	Barcelona	gp	Garmisch-Partenkirchen	hh	Hamburg
ju	Jungfraujoch	kb	Kühlungsborn	la	L'Aquila	lc	Lecce	le	Leipzig
li	Lisboa	lk	Linköping	mi	Minsk	mu	München	na	Napoli
ne	Neuchâtel	pl	Palaiseau	po	Potenza	th	Thessaloniki		

As a result of the quality assurance exercises a few caveats have to be added: the stations at Lisbon and Palaiseau had serious problems with the hardware setup. Only very few measurements from these stations can be used for the purpose of this project. At Palaiseau these problems have been solved meanwhile, at Lisbon the upgrade is still in progress. Other systems showed some technical problems as well which mainly reduced the useful range of the measurements. This will be discussed in more detail in WP3.

At the first EARLINET workshop there was general agreement that the project would greatly benefit from the addition of a Raman channel for all systems where this was considered possible. A joint action was organised to purchase the necessary filters and thus achieve better performance and a substantial reduction in price. This action was very successful, a number of systems has meanwhile been upgraded.

Thanks to the efforts of the group in Minsk it was also possible to bring another station into operation which is located in Belsk, Poland. The data are processed and analysed by the group in Minsk. From October 2000 this station provided additional measurements that are considered typical for a rural or background environment with no direct influence of industrial pollution. This will be very useful for the assessment of natural versus anthropogenic sources of aerosol over Europe.

### **3.1.3 Plans for the next period**

The work package is considered completed with very good success. The Lisbon station is expected to start regular measurements around May 2001. At some stations system upgrades will continue and thus improve the performance. In addition it has to be considered that the intensive use of the systems will inevitably cause some failures. So far only few breakdowns occurred. Fortunately the institutions managed to organise a repair on their own expense in rather short time, so that the general status is still considered excellent. We are confident that this will be true for the future, too.

## **3.2 WP2, Regular measurements**

by Jens Bösenberg

### **3.2.1 Objective**

The goal of this work package is the establishment of a comprehensive climatological database of the vertical distribution of aerosol over all stations of the network.

### **3.2.2 Methodology**

For the data set to become comprehensive and statistically significant in a climatological sense it is necessary to perform the measurements at a rather large number of stations under a broad range of atmospheric conditions. One of the important advantages of lidar over passive remote sensing methods is that it can yield reliable results even in case of the presence of complex cloud fields that are variable in height and horizontal extension. In order to avoid any bias in the results due to selection of specific conditions for the measurements, the climatological data set is collected on a regular schedule on preselected dates, regardless of weather conditions. If weather conditions do not permit lidar operation during the scheduled period, e.g. due to rain or fog, this fact is noted in the data record, thus providing a statistics of occasions when aerosols do not play a major role for most atmospheric processes. Based on the experience with the German aerosol lidar network it was resolved to schedule 3 measurements per week on 2 different days as a good compromise between requirements for good coverage and limitations of resources.

Specifically, measurements are made routinely on Mondays around 13:00 UT and around sunset, and on Thursdays around sunset. These times were selected to have one daytime measurement with a well developed boundary layer, and two measurements with low background light to benefit from the most advanced lidar methods that are best operated in the dark, and to make measurements of the dust layer that has developed during the day.

### **3.2.3 Scientific Achievements**

As stated before, almost all groups started regular measurements as scheduled and sent their reports to the coordinator. Table 3.2 shows the number of measurements for the months May to November 2000 that have actually been performed, successfully evaluated, and delivered to the data base, for all individual stations.

The performance is quite different for the stations, reflecting the facts that the existing systems do have different operational properties, that skills for operation and evaluation of lidar measurements are different, and that weather conditions can be quite different. In addition it has to be considered that in particular for Munich and Hamburg there was an extra work load for moving their systems to the intercomparison sites. Many systems show an excellent performance right from the beginning of the project, only few had serious technical problems. The overall performance appears to be about as expected, the number of missing measurements due to technical or manpower problems is acceptable.

Station scheduled	ab	at	ba	be	gp	hh	ju	kb	la	lc	le	li	lk	mi	mu	na	ne	pl	po	th
05/2000: 14	4	5	8	-	0	12	3	11	5	10	2	-	-	10	8	10	3	2	10	5
06/2000: 13	4	7	11	-	2	7	4	9	7	12	2	-	-	11	8	12	6	3	9	5
07/2000: 14	3	13	13	-	2	6	3	8	3	14	2	-	-	9	6	1	1	3	12	3
08/2000: 13	0	2	12	-	3	12	4	7	0	10	3	-	-	9	5	0	4	0	10	9
09/2000: 12	0	10	5	-	1	4	3	6	6	7	4	-	-	8	0	1	4	1	9	7
10/2000: 14	0	4	5	14	2	6	4	9	6	10	3	-	-	11	1	9	5	0	7	4
11/2000: 13	4	7	3	10	3	8	0	12	6	9	6	-	-	3	8	9	0	0	13	5
total: 93	17	48	57	24	13	55	21	62	32	72	22	-	-	61	36	42	23	9	70	38
performed %	18	52	61	89	14	59	23	67	34	77	24	-	-	66	39	45	25	10	75	41

ab	Aberystwyth	at	Athens	ba	Barcelona	be	Belsk	gp	Garmisch-Partenkirchen
hh	Hamburg	ju	Jungfraujoch	kb	Kühlungsborn	la	L'Aquila	lc	Lecce
le	Leipzig	li	Lisboa	lk	Linköping	mi	Minsk	mu	München
na	Napoli	ne	Neuchâtel	pl	Palaiseau	po	Potenza	th	Thessaloniki

Table 3.2: Overview over the number of performed measurements, per month and per station.

Specifically for the Linköping station it should be noted that a number of measurements has been performed, but the data have not yet been processed because of unexpected manpower problems. So there will be additional contributions to the data base. It should also be noted that for Jungfraujoch a special schedule has been adopted. Because of logistical reasons the station is operated only every other week, but with a high density of measurements during that time. This is considered appropriate for that special high altitude station that addresses mainly stratospheric aerosol.

### **3.2.4 Plan for the next period**

The regularly scheduled measurements will be continued as planned. It is expected that the performance of several stations will improve with the personnel becoming better trained and the systems becoming better equipped for routine operation and evaluation. According to the experience a yield of more than about 60% should be attainable for all stations except maybe for those with extremely bad weather statistics. For many stations this may be substantially exceeded.

## 3.3 WP3, Quality assurance

by Christine Böckmann and Volker Matthias

For the purpose of using data from different stations in joint studies, and for the reliability of the data base as a whole it is important that the data quality is checked independently from the efforts of the individual groups. Data quality depends on system hardware as well as evaluation software. Tests have been performed for both areas separately and for overall performance. These will be described in detail in the following two sections.

### 3.3.1 Algorithm intercomparison

#### Objectives

A basic exercise to assure the quality of network measurements is the comparison of the algorithms used to calculate the optical parameters from the lidar signals. Especially, the determination of the particle backscatter coefficient from a single elastic backscatter signal has to be proven. The general problem of the method to determine a quantity from a signal, which is influenced by two unknowns, may lead to differences between solutions obtained from different algorithms. Therefore, an intercomparison of algorithms applied by different lidar groups for retrieving the particle backscatter-coefficient profile was organized as part of the EARLINET Network. Using their individual algorithms all participating groups (except two groups) processed three sets of synthetic lidar data.

#### Methodology

Synthetic lidar signals were used for the algorithm intercomparison. In this way, the numerical correctness and accuracy of the algorithms as well as the experience of the groups and the limits of the method itself could be tested for examples with different degree of difficulty. The synthetic lidar signals were calculated by the IfT group with the IfT lidar simulation model. The simulations were performed by a person who was not involved in the evaluation of these data for the intercomparison study and the input data were not known to other persons. This software permits one to simulate and to evaluate elastically and inelastically backscattered lidar signals of arbitrary wavelengths in dependence on a variety of system parameters for a variable model atmosphere with arbitrary aerosol and cloud layers. Sky background, background noise, and signal noise are considered as well. Atmospheric input parameters are profiles of temperature and pressure to calculate Rayleigh scattering and profiles of extinction coefficients and lidar ratios for the simulation of aerosol and cloud layers. For the algorithm intercomparison three different data sets of elastic backscatter signals at wavelengths of 355, 532, and 1064 nm were simulated. A US standard atmosphere with a ground pressure of 1013 hPa and a ground temperature of 0 °C, a tropopause height of 12.0 km, and isothermal conditions above were assumed. Three different sets of elastic backscatter signals for realistic atmospheric conditions were computed. For the first example, the input profiles of extinction coefficient and lidar ratio were provided to the participants to allow an exercise with known solutions. Examples 2 and 3 were used for the intercomparison. In example 2, a wavelength-dependent extinction-coefficient profile was assumed and the lidar ratio was dependent on wavelength but constant with height. In contrast, for example 3 a height-dependent but wavelength-independent lidar ratio was used.

Most of the lidar inversion algorithms are based on the works of Fernald (1984) and Klett (1985). Because two unknowns, particle extinction and particle backscattering, influence the measured elastic backscatter signal, the algorithm considers a linear relationship between the extinction and the backscatter coefficient, the extinction-to-backscatter or lidar ratio. This input quantity is unknown in principle, because it depends on the actual physical and chemical properties of the atmospheric particles. In addition, a reference value is needed for the inversion, which usually is set into a height region, where Rayleigh scattering dominates the measured signal. Rayleigh scattering is calculated from temperature and pressure values of a radiosonde ascent or a standard atmosphere. Assuming a monochromatic laser pulse  $P_0(\lambda)$  at wavelength  $\lambda$ , the lidar signal  $P(\lambda, z)$  received during the integrating time  $\Delta t$  from the scattering of the laser light in the atmospheric layer located at altitude  $z$  is given by

$$P(\lambda, z) = C(\lambda)P_0(\lambda)\beta(\lambda, z)\frac{1}{z^2}\exp\{-2\int_0^z \alpha(\lambda, u)du\}, \quad (3.1)$$

with the backscatter coefficient

$$\beta(\lambda, z) = \beta^{Ray}(\lambda, z) + \beta^{Aer}(\lambda, z) \quad (3.2)$$

and the extinction coefficient

$$\alpha(\lambda, z) = \alpha^{Mol}(\lambda, z) + \alpha^{Aer}(\lambda, z) = \alpha_{abs}^{Mol}(\lambda, z) + \alpha_{sca}^{Ray}(\lambda, z) + \alpha_{abs}^{Aer}(\lambda, z) + \alpha_{sca}^{Aer}(\lambda, z). \quad (3.3)$$

The signal depends on the backscatter coefficients of molecules and aerosol particles  $\beta^{Ray}$  and  $\beta^{Aer}$ , respectively, and on attenuation due to molecular scattering  $\alpha_{sca}^{Ray}$  and absorption  $\alpha_{abs}^{Mol}$  and particle scattering  $\alpha_{sca}^{Aer}$  and absorption  $\alpha_{abs}^{Aer}$ .  $C$  is the system constant.

The determination of the aerosol backscatter coefficient  $\beta^{Aer}(\lambda, z)$  from the elastic backscatter signal of Eq. (3.1) requires the solution of a Bernoulli differential equation. As the result one obtains

$$\begin{aligned} \beta^{Aer}(z) = & \frac{P(z)z^2 \exp\left\{2\int_z^{z_0} [S^{Aer}(u) - S^{Ray}] \beta^{Ray}(u) du\right\}}{\frac{P(z_0)z_0^2}{\beta^{Aer}(z_0) + \beta^{Ray}(z_0)} + 2\int_z^{z_0} S^{Aer}(u)P(u)u^2 \exp\left\{2\int_u^{z_0} [S^{Aer}(v) - S^{Ray}] \beta^{Ray}(v) dv\right\} du} \\ & - \beta^{Ray}(z), \end{aligned} \quad (3.4)$$

with the lidar ratios of molecular and particle scattering

$$S^{Ray} = \frac{\alpha^{Ray}}{\beta^{Ray}} = \frac{8\pi}{3} \text{ and } S^{Aer}(\lambda, z) = \frac{\alpha^{Aer}(\lambda, z)}{\beta^{Aer}(\lambda, z)}, \quad (3.5)$$

respectively. Molecular absorption is neglected here. Molecular scattering can be calculated from

$$\alpha_{sca}^{Ray}(z, \lambda; P, T) = \frac{8\pi^3(m_{air}^2 - 1)^2}{3\lambda^4 N_s^2} \frac{6 + 3\gamma}{6 - 7\gamma} N_s \frac{T_0}{p_0} \frac{p(z)}{T(z)} \quad (3.6)$$

with the refractive index of the air  $m_{air}$ , the depolarization factor  $\gamma$  ( $\gamma$  is 0.0301, 0.0284 and 0.0273 for 350, 550 and 1000 nm, respectively), and the molecular number density  $N_s = 2.547 * 10^{19} \text{cm}^{-3}$  for standard atmospheric conditions at ground level ( $p_0=1013.25 \text{ hPa}$ ,  $T_0=15^\circ\text{C}$ , 0.03%  $\text{CO}_2$ ). Profiles of temperature  $T(z)$  and pressure  $p(z)$  are taken from actual radiosonde measurements or from a standard atmosphere with actual ground values of temperature and pressure. Two unknown quantities, the particle lidar ratio and the particle backscatter coefficient  $\beta^{Aer}(z_0)$  at a suitable reference

height  $z_0$ , have to be estimated in the determination of the particle backscatter-coefficient profile after Eq. (3.4).

Thus, the numerical schemes differ from each other only in minor details. Before Eq. (3.4) can be applied to measured lidar signals, the signals are averaged over the time interval of interest, corrected for background, and, if necessary, spatially averaged (smoothed). For the synthetic data used here, this procedure was not necessary.

## Scientific achievements

The procedure of the algorithm intercomparison was as follows. First, the simulated signals were distributed to all groups without any information on the input parameters, except the used standard atmosphere. The groups calculated particle backscatter-coefficient profiles with their individual algorithms and sent the solution to UPIM. The UPIM group is not involved in experimental lidar work and acted as the referee as well as took over the complete analysis.

This first stage was the most difficult and most realistic one, because lidar-ratio profiles and reference values were unknown. Therefore, not only the correctness and accuracy of the algorithms was proven but also the experience in estimating the lidar ratio and choosing the reference value.

In the second stage, the input lidar-ratio profiles were distributed and the groups had to evaluate the signals again. In the third and final stage, both lidar-ratio profiles and reference values were given to the participants.

Thus, the final stage proves definitively the numerical correctness, i.e., the accuracy and stability of the algorithms depending on the noise level and other circumstances as explained below. The results of each group from each step were compared with the input data in order to determine the systematic errors.

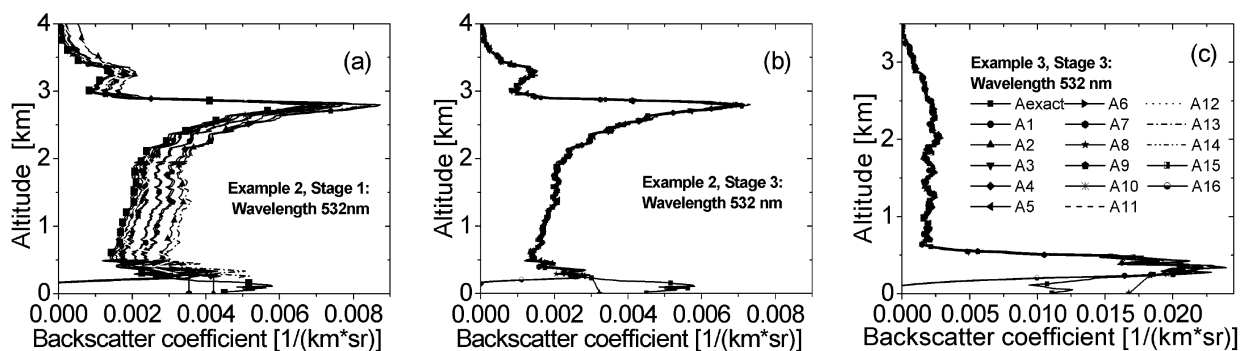


Figure 3.1: Backscatter coefficients at 532 nm calculated by the groups A1–A16 in comparison to the correct solution for (a) simulation case 2, stage 1, (b) simulation case 2, stage 3, and (c) simulation case 3, stage 3.

Figure 3.1(a) shows the backscatter-coefficient profiles at 532 nm for simulation case 2 obtained by the different groups in stage 1. The deviations from the correct solution were between 0% and 100%. In the second stage the lidar ratio was known, and in the third stage both input values were given to the participants. Thus, the final stage proves definitively the numerical correctness, i.e., the accuracy and stability of the algorithms. The results of stage 3 for simulation cases 2 and 3 are shown in Fig.3.1(b) and (c), respectively.



## Discussion and conclusion

The algorithm intercomparison showed that in general the data evaluation schemes of the different groups work well. Differences in the solutions can mainly be attributed to differences in the estimate of the input parameters. If the input parameters are known, remaining errors are of the order of a few percent. The unknown lidar ratio had the largest influence on the solutions, which again demonstrates the need for independent measurements of the particle extinction coefficient, e.g., with the Raman method. The unknown reference value was of minor importance for the examples presented here, because height regions with dominating Rayleigh scattering were present in all cases. It should be mentioned, however, that this is not necessarily the case under atmospheric conditions. Especially at 1064 nm, particle scattering often dominates the signals in the entire measurement range, which may cause additional errors that were not discussed here. Differences in the solutions can mainly be attributed to differences in the estimate of the input parameters. If the input parameters are known, remaining errors are of the order of a few percent. The unknown lidar ratio had the largest influence on the solutions.

## Plan and Objectives for the next period

To overcome the problem of an unknown lidar ratio, independent measurements of the particle extinction coefficient with the Raman method are or will be performed at most of the network stations. Therefore, a second algorithm intercomparison is in preparation.

The sources of uncertainties in the determination of the aerosol extinction coefficient from Raman signals are represented by:

- (a) the statistical error due to signal detection (Theopold and Bösenberg, 1988);
- (b) the systematic error associated with the estimate of temperature and pressure profiles (Ansmann et al., 1992);
- (c) the systematic error associated with the estimate of the ozone profiles in the UV (Ansmann et al., 1992);
- (d) the systematic error associated with the wavelength dependence parameter  $k$  (Ansmann et al., 1992; Whiteman, 2000);
- (e) the systematic error associated with the multiple scattering (Ansmann et al., 1992; Wandinger, 1998; Whiteman, 2000);
- (f) the error introduced by operational procedures such as signal averaging during varying atmospheric extinction and scattering conditions (Ansmann et al., 1992; Bösenberg, 1998).
- (g) For a correct application, it is necessary to calculate the derivative of the logarithm of the ratio of two quantities, i.e. the atmospheric number density  $N(z)$  and the range-corrected  $N_2$  Raman lidar signal ( $z^2 P(z)$ ).

The derivative is usually performed through a least-squares technique, by fitting the Raman lidar data by means of linear or quadratic functions. For a correct statistical approach to the problem, the  $\chi^2$  confidence test has to be used to assess both the best model and the measurement error (Whiteman, 1999). The careful application of statistical analysis techniques is required to accurately estimate the aerosol extinction and the aerosol extinction error.

The IfT-group already prepared two files with simulated Raman signals. The signals correspond to the EARLINET training case Example 1. The simulated Raman signals have different shot noise and are simulated without background/background noise.

### **3.3.2 Instrument intercomparison**

The second part of the quality assurance within the EARLINET project are the intercomparisons of the lidar systems. For this purpose, a variety of simultaneous measurements should be taken at one place at different times and under different meteorological conditions. The calculated backscatter profiles should be compared to each other to prove the performance and also the reliability of the systems.

#### **Experiments**

12 of the lidar groups performed two major experiments during September and October 2000. The mobile lidar system of the Ludwig-Maximilians-Universität München travelled to Italy and Greece in September and October 2000 and made intercomparisons with the groups from Athens, Thessaloniki, Lecce, Potenza, Napoli and L'Aquila. The groups from Barcelona, Hamburg, Lisbon, Neuchatel and Palaiseau met at the Ecole Polytechnique in Palaiseau between 11 September and 14 September.

Additional experiments have been performed in October 2000 in Hamburg (intercomparison with Linköping) and in Neuchatel (intercomparison of the mobile micro lidar with the three wavelengths lidar). In January 2001 the Munich lidar performed intercomparisons with Garmisch-Partenkirchen. Considering that four of the German lidar groups already did such intercomparison experiments in the frame of the German Lidar Net in 1998, only three groups have not yet compared their systems. The EPFL-lidar, which is located on the Jungfrauoch will do their intercomparisons in March 2001 and the lidar from Aberystwyth will be compared to Hamburg in May 2001.

With respect to the systems in Minsk and Belsk no possibility has been found up to now to perform direct system intercomparisons. This is mainly due to customs and logistical reasons. The best possibility to assess data quality is the use of extensive internal tests and repeated plausibility checks of the results.

#### **First results**

First results of the aerosol backscatter measurements at 532 nm and 1064 nm have already been compared in Palaiseau to check whether systematic errors occurred and changes in the system configuration would be necessary. The Hamburg aerosol Raman lidar compared successfully to the Neuchatel micro lidar at 532 nm and to the Barcelona backscatter lidar at 1064 nm. Several examples from different days are shown here (figures 3.2 to 3.3).

The profiles have been evaluated with common boundary values and lidar ratios, so errors due to lack of information (e.g. lidar ratio) or different experience in estimating calibration values have no

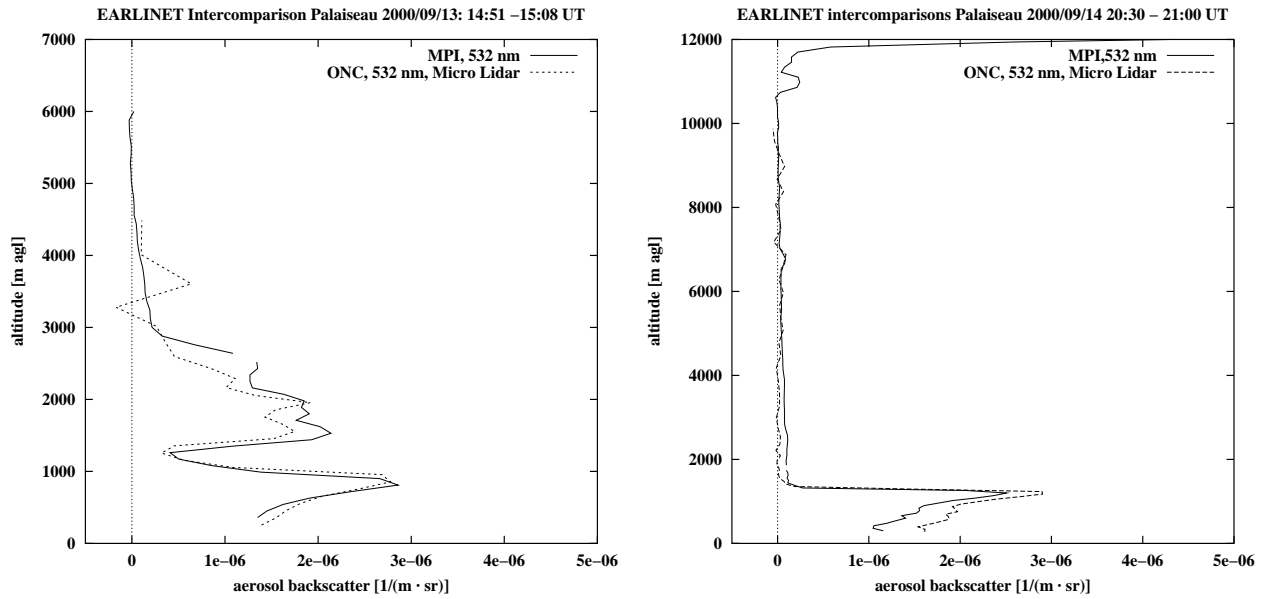


Figure 3.2: Intercomparison of aerosol backscatter at 532 nm between MPI Hamburg and Observa-tory Neuchatel.

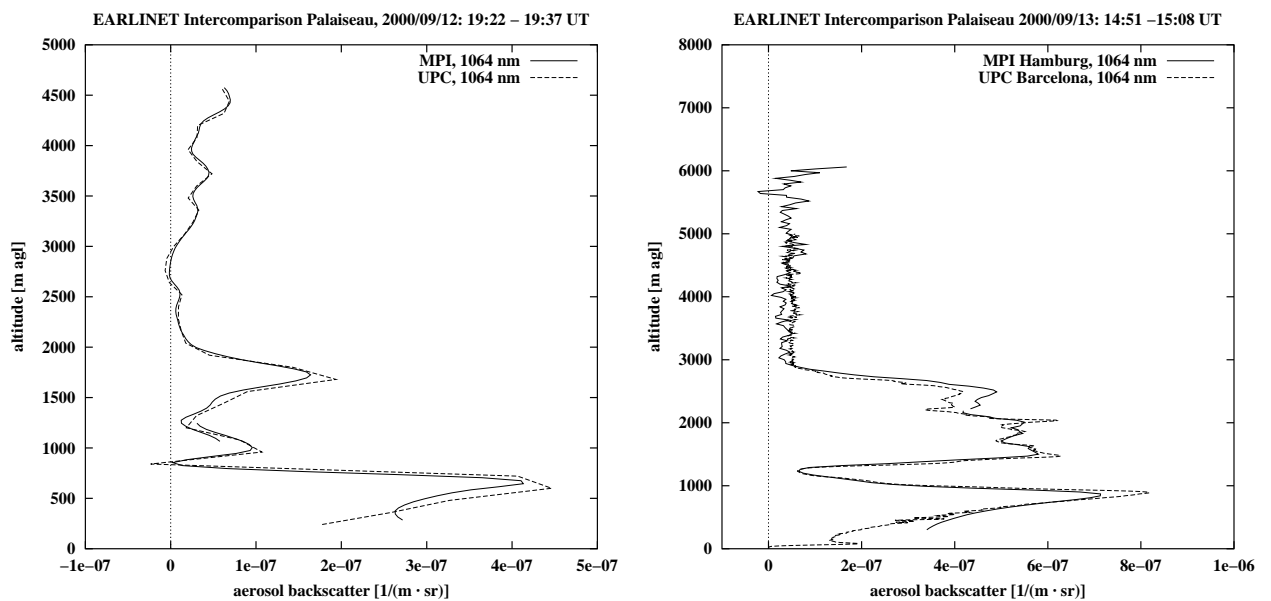


Figure 3.3: Intercomparison of aerosol backscatter at 1064 nm between MPI Hamburg and UPC Barcelona.

influence on the results. The used algorithms have been proven (see this workpackage) so additional errors caused by the algorithms can be neglected.

The profiles generally show good agreement. The daytime measurements of the Neuchatel micro lidar are limited in range due to the high background light, but the main aerosol structures can be measured although the output energy is very low.

The profiles derived by the UPC Barcelona at 1064 nm show little higher noise in the upper part of the atmosphere than the MPI profiles do, since they use a relatively small receiving mirror of ca. 20 cm diameter and the MPI uses a mirror of 50 cm diameter for the upper range measurements.

Although these intercomparisons show the high quality that can be achieved with aerosol backscatter measurements by lidar, problems occurred with the lidar systems from Lisbon and Palaiseau. The Lisbon system suffered from a hardware damage of the data acquisition that occurred during the transport of the system. It took three days to fix this problem and after that some measurements could be made. The detected signal was quite low and it was seen that the receiver field of view was much too narrow to perform measurements in the boundary layer. To get a wider field of view, the 200  $\mu\text{m}$  diameter glass fibre in the focus of the receiving telescope has to be changed to a bigger one, which could not be done during the experiment.

The measurements performed with the Palaiseau lidar system showed a misalignment of the laser beam relative to the field of view of the receiving telescope. Further tests showed that the system, which is equipped with a large receiving telescope of 60 cm diameter is not suitable for measurements in the boundary layer. The lowest altitude with full overlap between laser beam and telescope field of view was in ca. 3000 m, so only upper tropospheric measurements could be used for the intercomparisons. Measurements under this configuration have been done at only one day.

Besides this experiment covering five groups, the Munich mobile aerosol lidar system travelled to Greece and Italy and performed intercomparisons with the two groups in Greece and the four groups in Italy at their sites. Several measurements have been done in each city under different conditions, however sometimes bad weather prevented bigger data sets.

Generally good agreement could be achieved in the upper part of the troposphere but problems occurred in the near range with some of the systems. One example can be seen in figure 3.4, where the Thessaloniki lidar clearly shows too low values in the near range. These problems could be assigned to detector saturation since the system works in photon counting mode and too high count rates lead to saturation effects.

Similar problems occurred with the lidar from Athens. Good results have been achieved in heights above 1500 m, below that height mainly detector saturation effects prevented better performance of the NTUA lidar during the intercomparisons.

The L'Aquila lidar works with full overlap between receiver field of view and laser beam in altitudes of ca. 4 km. Aerosol backscatter coefficients below that height can only be evaluated using the Raman technique, where the overlap function cancels out in the equations. However this restricts measurements to nighttime, when the Raman signals can only be detected and prevents accurate intercomparisons. Using the Raman technique, the height dependent lidar ratio is implicitly given and cannot be derived from the measurement. So the measurements can only be compared to aerosol backscatter profiles from the Munich lidar calculated with different lidar ratios, not knowing which the correct one would be. Having these restrictions in mind the comparisons were satisfying down to low altitudes within the PBL.

Problems in the near range up to ca. 1000 m above ground were also present in Potenza and in Lecce. In Potenza the problems were mainly assigned to stray light in the receiving channels while in Lecce the slit width of the used spectrometer defines the field of view of the telescope and therefore the lowest height with full overlap.

Good results in the UV have been achieved in Napoli, also down to ca. 300 m above ground. Up to now only range corrected signals have been compared, but backscatter profiles will probably show only small deviations. They will be calculated and compared for the main report.

Examples of these measurements can be seen in the figures 3.5 - 3.9.

The MPI Hamburg and the FOA Linköping compared their systems at UV wavelengths in October 2000 in Hamburg. Also in this case, good agreement could be found in the upper part of the troposphere, but in the near range considerable deviations have been found. Most likely they were also due to detector problems of the Linköping lidar, which additionally operates with a too narrow field

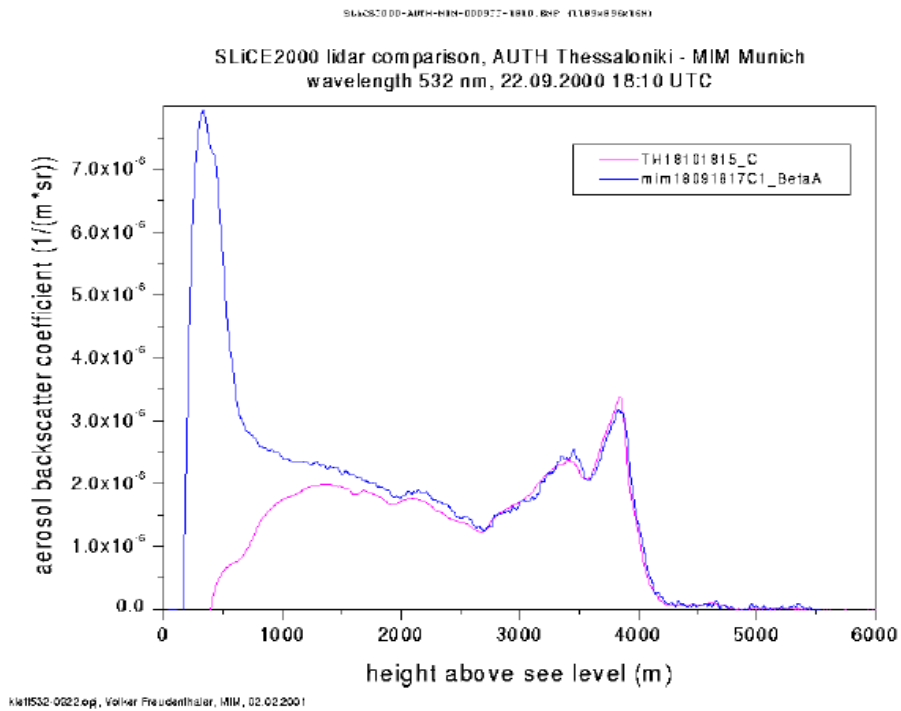


Figure 3.4: Intercomparison of aerosol backscatter at 532 nm between MI Munich and AUTH Thessaloniki.

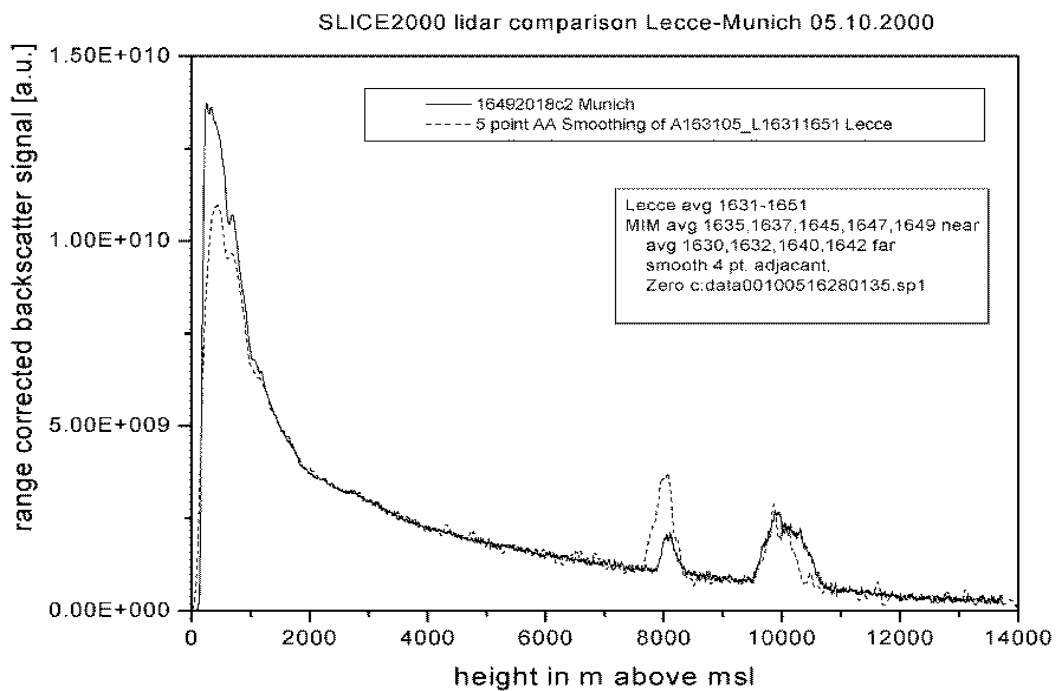


Figure 3.5: Intercomparison of  $Pr^2$  between MI München at 355 nm and INFM Lecce at 351 nm.

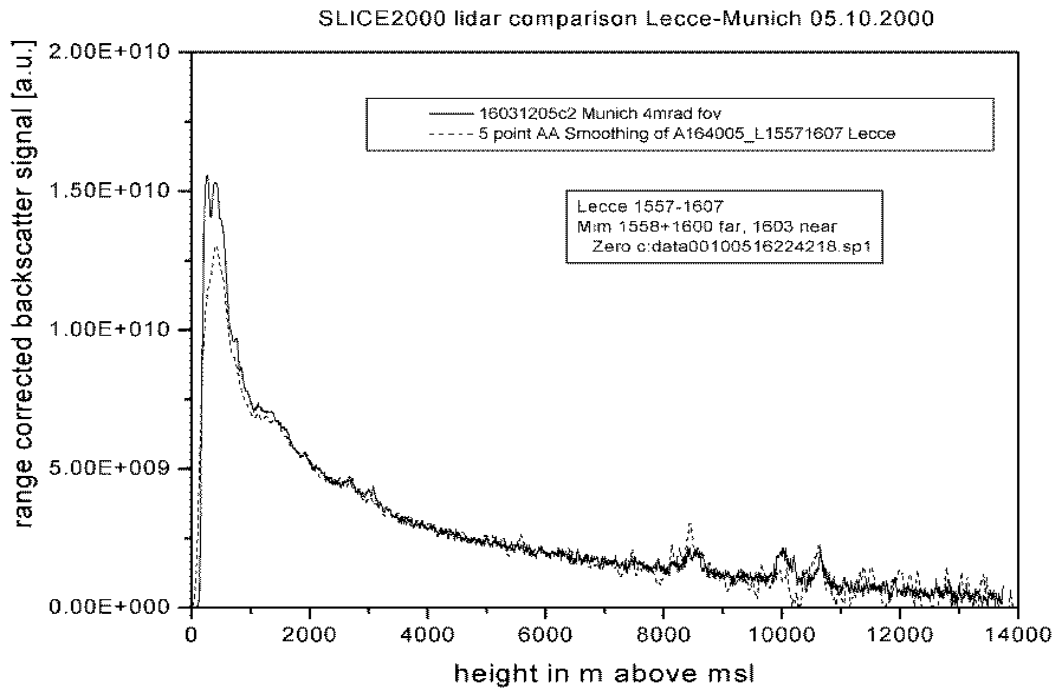


Figure 3.6: Intercomparison of  $Pr^2$  at 355 nm between MI Munich and Lecce.

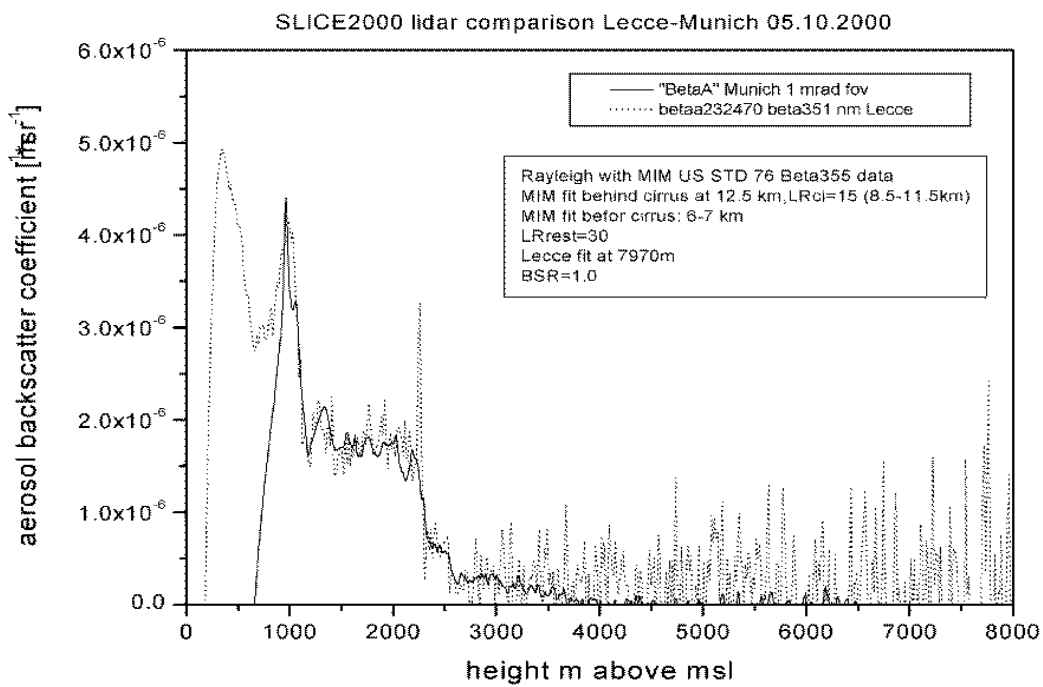


Figure 3.7: Intercomparison of aerosol backscatter at 355 nm between MI Munich and Lecce.

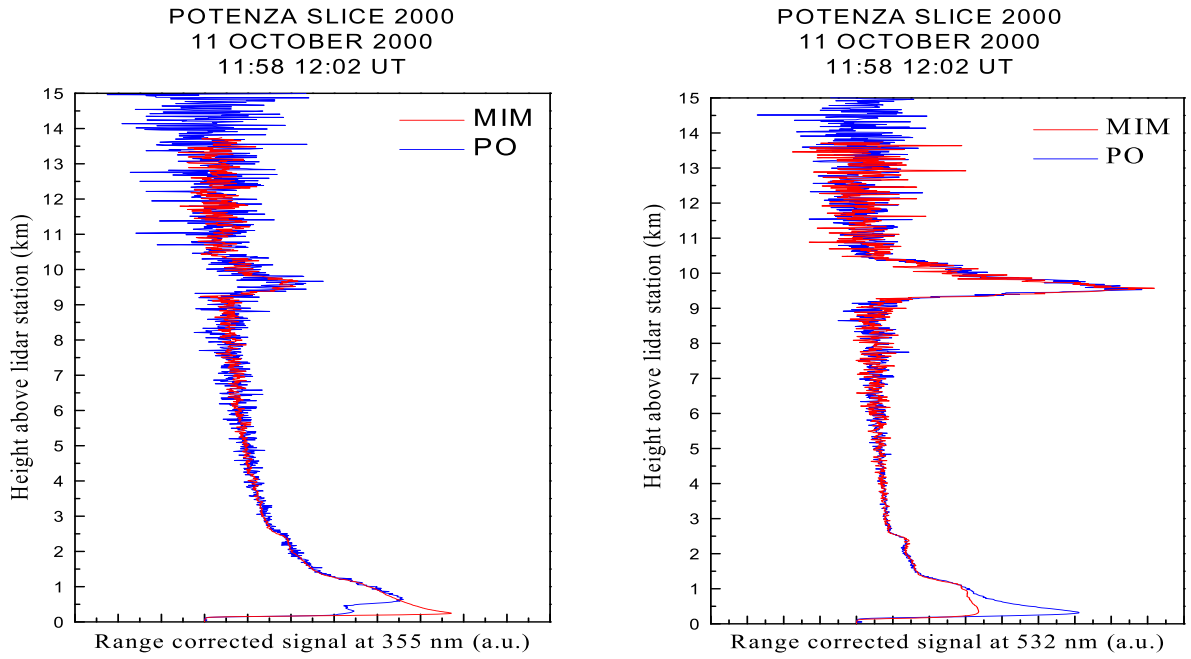


Figure 3.8: Intercomparison of  $Pr^2$  at 355 nm and 532 nm between MI Munich and Potenza.

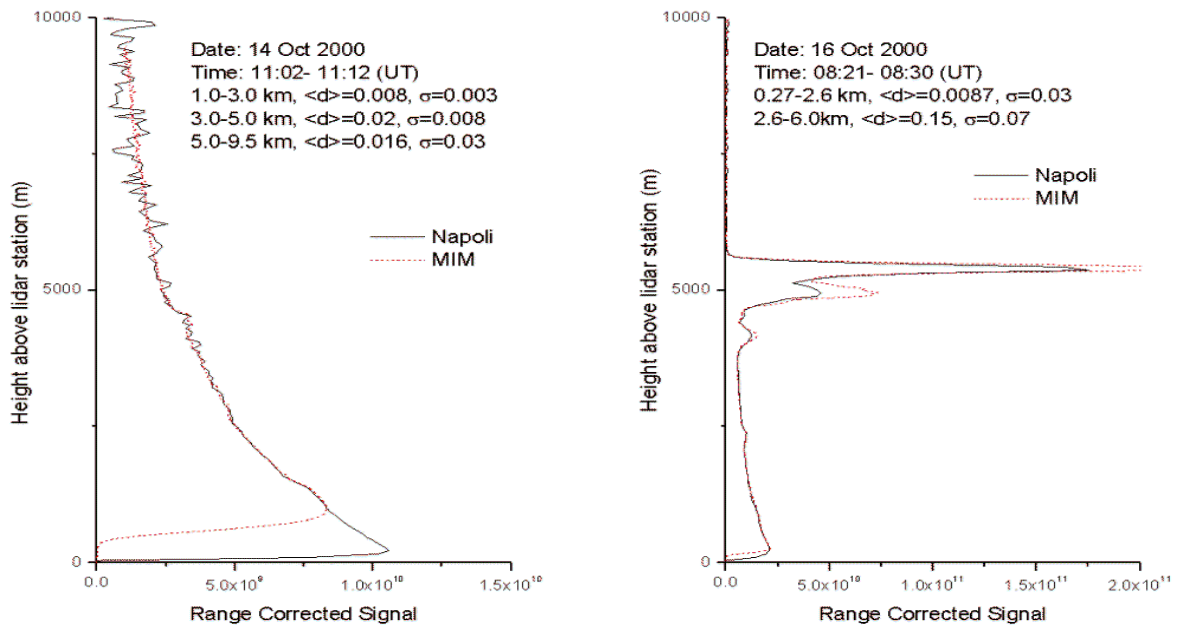


Figure 3.9: Intercomparison of  $Pr^2$  between MI München at 355 nm and INFN Napoli at 351 nm.

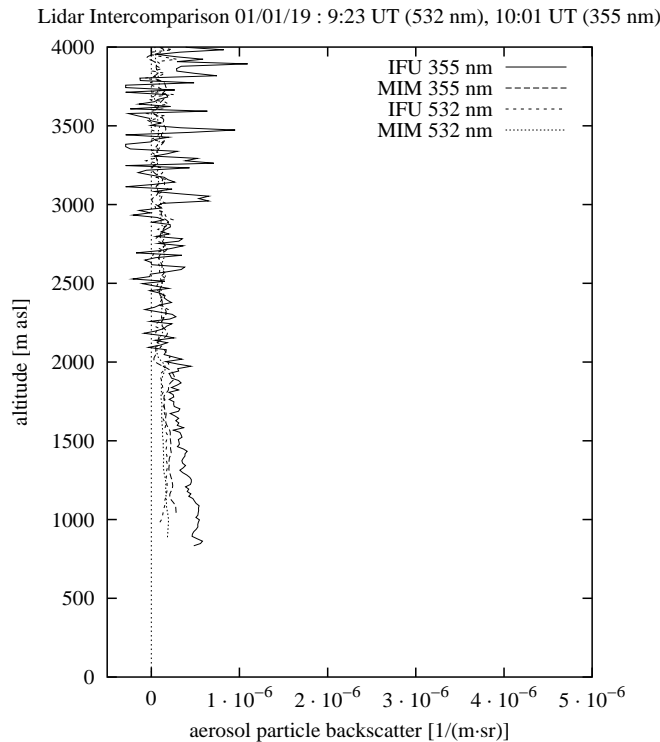


Figure 3.10: Intercomparison of aerosol backscatter at 355 nm and 532 nm between MI Munich and IFU Garmisch-Partenkirchen.

of view of the receiving telescope. Therefore it was decided to change the coaxial emitter/receiver configuration to a biaxial and use a larger aperture as field stop. This reconstruction was planned for the winter in Linköping to have additional measurements in early summer 2001.

An intercomparison between IFU Garmisch Partenkirchen and MI München has been done on 19 January 2001. Although the deviations between the range corrected signals were quite low at 355 nm and 532 nm, the intercomparison was only partly successful. On that day, the very low aerosol content in the atmosphere made comparisons of the aerosol backscatter very difficult.

### Consequences

Deviations between the measured aerosol backscatter profiles have been detected mainly in the near range for some of the compared systems. In all cases the reasons for these deviations have been found and most groups have already taken measures to avoid these problems after the intercomparison measurements.

In L'Aquila main reconstructions would be necessary to achieve full overlap well below 1000 m. However, since the aerosol backscatter profile can be determined down to ground using the Raman technique, the configuration will not be changed immediately.

The LMD Palaiseau installed in the meantime an additional lidar for the boundary layer operating at 532 nm. The system used for the intercomparisons remains for the upper part of the troposphere and will be equipped with a second small receiving telescope to get the lowest measurement range down to 300 m. Additionally, they started investigations on the experimentally derived overlap function of the upper troposphere lidar to correct for the incomplete overlap of the already taken routine measurements.

For the IST Lisbon it was decided to do the necessary reconstruction in Lisbon and repeat the in-



tercomparison experiment afterwards. The suggestion was that the Lisbon system should travel to Barcelona in spring 2001. Almost the same proceeding is planned for the intercomparisons between FOA Linköping and MPI Hamburg. The Swedish system will come to Hamburg in spring 2001 after the necessary changes in the configuration have been made.

The problems that occurred in Greece and Italy are believed to be minor ones and solvable by the groups themselves, without the need for further system intercomparisons. Here mainly data acquisition and data processing will be improved.

For the lidar at Garmisch-Partenkirchen additional intercomparisons are planned to have more than one single case and to cover a broader range of aerosol distributions. The system is very compact and easy to move, so further measurements of the Garmisch system in Munich can be done with acceptable effort.

## **Conclusions**

Most of the lidar systems operated in the EARLINET have already performed intercomparison experiments. Generally good results can be found in altitudes above 1.5 km, however also in the near range reliable measurements are necessary to achieve the goals of EARLINET. Measures have already been taken at several stations, namely Athens, Thessaloniki and Potenza to get better results in the boundary layer. No additional measurements to compare the lidars in Italy and Greece are necessary.

The situation was different for the lidars from Palaiseau and Lisbon. Here no satisfying results could be achieved and main changes in the system configuration were regarded to be necessary. These systems will do additional measurements in spring or early summer 2001 to prove their data quality after the reconstructions have been done. The same holds for Linköping (measurements in early summer in Hamburg) and Garmisch-Partenkirchen.

Besides the repetition of some of the intercomparisons, the first intercomparison of the University of Aberystwyth lidar system is already scheduled for the beginning of May 2001. The MPI Hamburg will travel to Wales and perform measurements during one week.

## 3.4 WP4, Compilation of trajectory data

by Ina Mattis

Atmospheric backtrajectories provide information about the origin of observed aerosols. Thus they are a very useful tool for the interpretation of measured lidar profiles of optical aerosol properties for special events like long-range aerosol transports [Bösenberg, 2001, Chapter 8.5], stable high-pressure situations [Bösenberg, 2001, Chapter 8.1] or cold front passages [Bösenberg, 2001, Chapter 8.2]. Further analytical trajectories can be used not only for the interpretation of special events, but also to perform climatological studies since atmospheric trajectories reflect the synoptic patterns corresponding to the measurements [Bösenberg, 2001, Chapters 6, 7.3, and 7.2]. Prognostic backtrajectories are a useful tool to organize coordinated intensive measurement periods or measurements of special events. Such prognostic trajectories are helpful in particular for the workpackages WP7 and WP9.

### 3.4.1 Atmospheric trajectories for the EARLINET project

The atmospheric trajectories, which are used for the EARLINET project, are calculated by the German Weather Service for all EARLINET lidar sites for two arrival times each day, which correspond approximately to the times of the routine lidar observations at noon and at sunset. The analytical as well as the prognostic trajectories are 4-day backward trajectories and are calculated from the wind fields of the global numerical weather prediction model of the German Weather Service [Kottmeier and Fay, 1998]. They are available since May 2000 for all EARLINET participants. The trajectories are calculated on a 3-dimensional grid. This calculation method leads to lower uncertainties in comparison to those of other methods, e.g. isentropic calculation. The accuracy of the calculated trajectories depends on the synoptic conditions. The higher the wind speed the lower the uncertainty of the trajectories. Usually the deviation between the calculated and the actual track of an air parcel is about 10% to 20% of the trajectory length for the trajectories used in this study [Stohl, 1998]. The characteristic properties of the trajectories are summarized in table 3.3.

The trajectories are stored in a data base at the IfT Leipzig. All EARLINET partners have access to that trajectory archive via an interactive web page (<http://earlinet.tropos.de:8084>). A visualization software for trajectories, which was developed at the IfT is as well available. Figure 3.11 shows an example of a complete data set of analytical trajectories. This example clearly demonstrates, that trajectories provide more information about the origin of observed air masses than only profiles of the wind direction at the measurement site. The 500-hPa trajectory originates in the Mediterranean region but reaches the measurement site from the north. This example further illustrates, that the observed aerosols at different height levels may have completely different sources. The boundary-layer aerosol measured on this day was advected from eastern Europe (see trajectories arriving at 975 and 850 hPa). But there were also aerosol layers in the free troposphere, which came from the Mediterranean region and from the African continent (see trajectories at 770 and 500 hPa).

### 3.4.2 Statistical analysis of trajectories

Because the quantity of available trajectory data sets (two per day) is much larger than the number of measured aerosol profiles (usually not more than three per week), we suggest to apply any method of statistical analysis primarily to the trajectories and not directly to the lidar profiles. Since the

trajectory model		
data base	Global numerical weather prediction model of the German Weather Service	
spatial resolution	1.5 deg	
time resolution	6 hr	
trajectory length	4 days	
available trajectory data set		
	analytical trajectories	prognostic trajectories
arrival times	13 UTC 19 UTC	13 UTC subsequent day 13 UTC 2 days later
arrival pressure levels	975 hPa 850 hPa 700 hPa 500 hPa 300 hPa 200 hPa	850 hPa 700 hPa

Table 3.3: Characteristical properties of the trajectories calculated by the German Weather Service for 20 EARLINET lidar sites.

analytical trajectories provide information on the synoptic patterns corresponding to the measurements, they should be used to classify profiles of optical aerosol properties derived by the routine observations in dependence on the large-scale weather regime as described in [Mattis et al., 2001]. For that purpose, the trajectories will be divided into distinct clusters by means of cluster analysis. Then each lidar profile can be assigned to the cluster of its corresponding trajectory. Because a trajectory cluster represents one large-scale atmospheric transport pattern, each of the profiles within the corresponding class of optical aerosol properties was obtained from a lidar observation under similar large-scale synoptic conditions. Investigations of the properties of these aerosol classes will show the dependence of optical aerosol properties on the corresponding weather regime.

Cluster analysis provides algorithms to separate a large number of data sets (in our case sets of trajectories) into groups, the so-called clusters. The separation of the data sets has to be done in such a way that similar trajectories are merged within one cluster and dissimilar ones belong to different clusters. In this study, a clustering algorithm for atmospheric trajectories recommended by [Dorling et al., 1992] was used. Modifications concerning the starting conditions provide additional information on the uncertainty of the derived results. As an advantage of the used clustering algorithm, the optimum number of clusters follows from the algorithm itself and does not have to be assumed.

The algorithm starts with the generation of about 30 seed trajectories. Modifying Dorlings algorithm synthetical rather than real trajectories were used. Then each trajectory is assigned to that seed, which is closest in terms of the used measure of distance and the average trajectory of each group is calculated from all group members. These mean trajectories are the so-called centroids. The next step is an iteration, which checks whether each real trajectory is in the right cluster in terms of its distance to the clusters centroid. The iteration reorganizes the trajectories if necessary and recalculates the centroids until all trajectories are correctly assigned.

To obtain the optimum cluster number the algorithm iterates decreasingly over the number of clusters  $N$ . Within each step,  $N$  is reduced by merging those two clusters, for which the centroids are

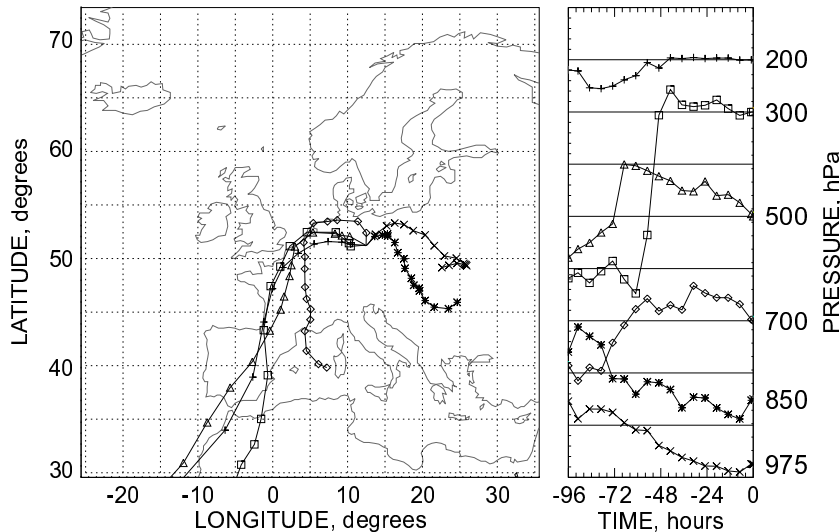


Figure 3.11: 4-day backtrajectories arriving at Leipzig as example for the data sets, which are calculated by the German Weather Service for 20 EARLINET lidar sites.

closest. Then the trajectories are iteratively assigned to the clusters as described before. The Root Mean Square Deviation ( $RMSD$ ) of each trajectory from its centroid is calculated. The sum of these  $RMSDs$  gives the total  $RMSD$ . The reduction of  $N$  leads in general to a weak increase in  $RMSD(N)$ . A steep increase in  $RMSD(N)$  is observed when significantly different trajectories formerly located in distinct clusters are merged into one cluster. So the optimum number of clusters is the  $N$  before the steep increase in  $RMSD(N)$ .

To get an estimation on the uncertainties of this clustering procedure, Dorlings algorithm was extended toward a repetition of the initialization and iteration over  $N$  with slightly varied seed trajectories. The results of the clustering algorithm for the different initial conditions converge for a certain  $N$  ( $N_{con}$ ). For  $Ns$  larger than  $N_{con}$ , no stable clusters can be found and any peaks in the percentage change of  $RMSD$  for more than  $N_{con}$  clusters should be neglected in the search for the optimum number of clusters.

### 3.4.3 First results of cluster analysis of trajectories

The cluster analysis described above was applied to the trajectories of three years, which end at 850 hPa for the 5 German EARLINET lidar sites [Bösenberg, 2001, Chapter 6]. Trajectories are available for these arrival sites since 1998 in contrast to the other EARLINET stations, for which trajectory data were calculated only since May 2000. The 850-hPa trajectories are believed to be most representative for the main air transport in the upper part of the atmospheric boundary layer. The trajectories arriving at 975 hPa are more influenced by the earth surface and therefore their uncertainty is larger. Nevertheless, the cluster analysis was also applied to trajectories arriving at Leipzig at 975 hPa simply to give an example and an idea about the conditions in the lower boundary layer.

The optimum number of clusters was found to be five for almost all of the cases. The cluster patterns are very similar for the five locations and also for the two different pressure levels. Figure 3.12 illustrates how the trajectories of 1998, 1999, and 2000 are assigned to the five clusters identified by the clustering algorithm for the station Leipzig and both pressure levels. The five clusters represent

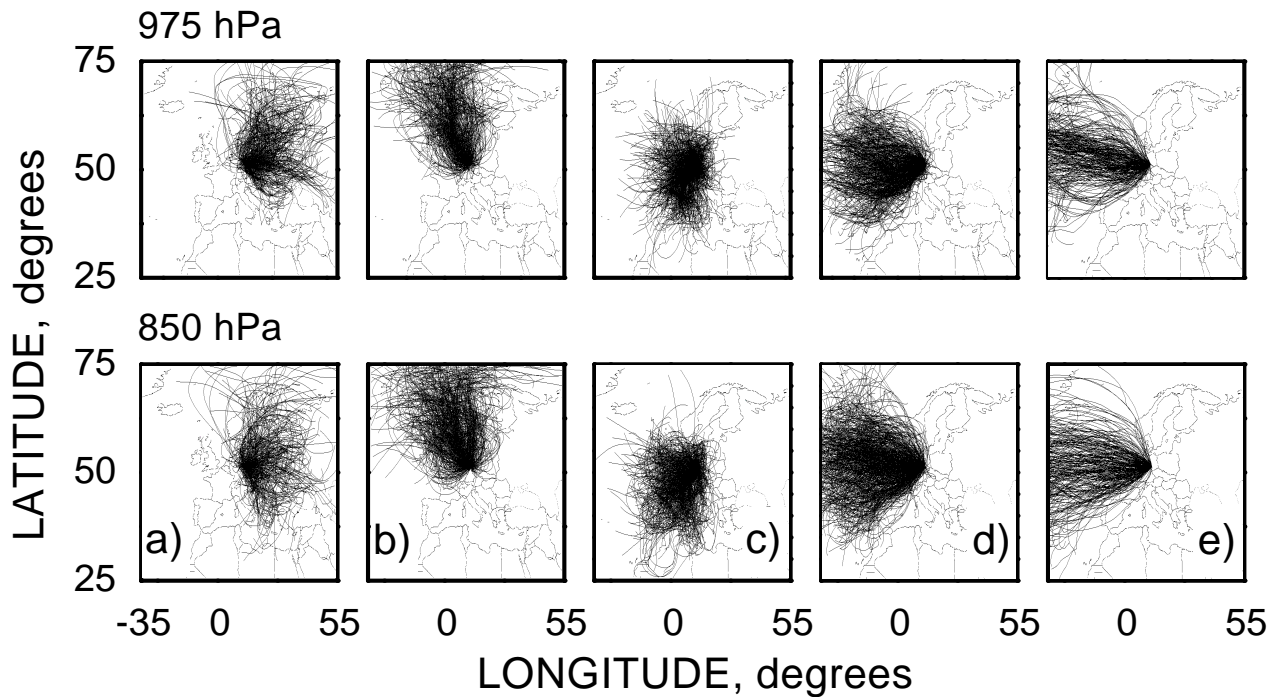


Figure 3.12: All trajectories of 1998, 1999, and 2000 arriving at Leipzig at 975 hPa (top) and 850 hPa (bottom) in the five clusters identified by the clustering algorithm. The characters in the lowest row identify the clusters.

weather regimes with different wind directions and speeds. Cluster a) contains all trajectories coming to Germany from easterly directions with low speeds. Air parcels which were transported to central Europe from northwest with higher wind speeds are merged within cluster b). Cluster c) combines trajectories from the Mediterranean Sea and very slow ones from western Europe. Those trajectories, which have their origin over the Atlantic ocean are combined in clusters d) and e) with the latter one characterized by very high wind speeds.

### 3.4.4 Conclusions

In the preceding section a method was introduced, which allows to classify profiles of optical aerosol properties derived by the routine observations in dependence on the large-scale weather regime. This method was first applied to trajectory data set for the past 3 years for the German lidar sites. As soon as the quantity of available EARLINET trajectories is large enough the cluster method will be applied to the other lidar sites, too.

Changing the used measure of distance in the clustering algorithm will allow to examine other questions than only the dependence on large-scale weather regime. Increasing the weight of the distance between two trajectories with decreasing distance to their arrival site will cause the algorithm to combine those trajectories into one cluster, which have crossed the same aerosol sources near the arrival site even if they originated from different regions. This tendency may be amplified by inserting any information about the surface below the trajectories (for instance emission maps) into the measure of distance.

## **3.5 WP5, Compilation of aerosol profile data**

by Holger Linné

### **3.5.1 Objectives**

The goal of this work package is the establishment of a large data base on aerosol profiles in a way that allows for easy access and automated processing of the results from all different stations.

### **3.5.2 Methodology**

A statistical analysis of a large data set requires automated processing of files originating from many different stations. Therefore it is a crucial requirement that a common format is used by all parties. Netcdf was chosen as a platform-independent, self-describing format that offers sufficient flexibility for later additions as they become necessary.

### **3.5.3 Scientific achievements**

The introduction of netcdf as a common data format was quite successful after some initial problems. All groups have submitted their evaluated profiles in this format to the common data base. The exchange of data files using a common protocol turned out to be more difficult as expected, mainly because of interference with computer security measures that are handled very differently at different computer centers and to some degree are mutually exclusive. Through intensive bilateral discussions solutions have been found for most groups. The result is a mix between a distributed data base which is maintained by the individual contributors, and a central data base at the MPI for those groups that cannot provide easy access for all partners to their data. All data are stored at the institution that has performed the measurements. Many institutions can provide direct internet access to the data for all EARLINET participants. For the other institutions the MPI has provided an ftp-site where the data can be put by the originator and subsequently are made public to the EARLINET community. For the first seven months the data from both the regular and the special measurements have been collected at the MPI and stored on a CD-ROM which can be provided upon request. This data set consists of roughly 3000 individual profiles of aerosol extinction or backscatter. This is by far the most extensive data set on aerosol vertical distribution, worldwide. It is certainly a great success that the common data set is already used by other work packages ( e.g. WP7, WP15) for scientific analyses.

### **3.5.4 Plans for the next period**

The collection of data will continue as scheduled. No major changes in the data format are foreseen, except an addition for continuous measurements over extended periods of time. Acces to the data for all partners and authorised external users will be maintained.

## **3.6 WP6, Temporal cycles**

by Jacques Pelon

### **3.6.1 Objectives**

The objective of the work to be performed in this WP is to obtain a significant set of observations of the aerosol properties in the lower troposphere at different time scales. Two main scales are aimed at, namely the day to day and the seasonal variation. This encompasses the diurnal and seasonal cycle of the aerosols in the boundary layer linked to its development as induced by solar and synoptic forcing.

Temporal variations due to special events such as the transport of aerosols linked to the occurrence of fronts, the seasonal transport of desert dust or of particles produced by biomass burning and production due to photochemical pollution are subject of a separate work package.

### **3.6.2 Methodology and scientific achievements**

All groups but one are involved in this work package. The main focus of this WP is put on the aerosol in the planetary boundary layer (PBL). The terminology boundary layer means the atmospheric layer directly coupled with the surface in a dynamical way over a diurnal cycle. However, in our analysis we also include the residual layer observed above the boundary layer during the day as a result of growth cycles over the previous days. Aerosol properties are different in both layers helping characterising the difference between the various layers.

Periods of observations are related to unperturbed weather conditions, ideally in a high pressure system. This allows to favour simultaneous observations at different stations and quantify the behaviour of aerosol at the regional scale.

The accumulation of the aerosol load during the day is depending on the aerosol source itself (natural or man-made), surface wind speed (dynamic forcing), and solar flux (thermal forcing) leading to turbulence development. The vertical stability (linked to the potential temperature gradient) and synoptic forcing are critical to the development of the boundary layer, and may lead to an increase of aerosol particles and pollutants when the growth of the boundary layer is blocked. The variation of the optical properties of the aerosols which is observed by lidar is further depending on moisture. The development of the boundary layer could thus be identical at different places or for several days, but the optical properties may differ.

During the morning, the growing boundary layer is eroding the stable and residual layers of the previous night and day, respectively. In the evening, the detrainment of the PBL and the sedimentation of large particles occurs during the stabilisation of the residual layer. In both transition phases the profile of the extinction coefficient is not constant with altitude. Morning transitions are important as particles and pollutants formed during daytime can be stored in the upper part of the residual boundary layer and further transported (possibly in the middle or upper troposphere, this topic is linked with WP12). During the formation of the stable nocturnal layer, this layer may include less particles and pollutants as no photochemical production will occur. The erosion of the residual layer above it during the following cycle may lead to a pollution increase near the surface, as the residual layer is mixed with the new growing active boundary layer. The structural and optical properties of these aerosol layers are thus important to be measured especially in the transition phases. This is made easier by the fact that this can be achieved in night-time periods, where Raman lidar can be operated.

Institute	Measurements	Wavelength	Date and time
IPSL Palaiseau France		532, 1064	02/06 : 07.25 - 17.33 07/06 : 07.45 - 23.16 08/06 : 09.00 - 18.22 09/06 : 07.42 - 16.47 19/06 : 06.29 - 13.49 20/06 : 06.16 - 16.04 19/07 : 07.24 - 18.41 30/07 : 08.20 - 16.26 31/07 : 07.15 - 17.38 01/08 : 06.12 - 16.30 14/09 : 07.20 - 20.30
IFT, Leipzig Germany		355, 532, 1064, 387, 607, 407	ftp site
NTUA, Athens Greece		532  355, 532 355, 387	29/05 : 08:25 - 09:33 29/05 : 14:57 - 18:15 16/11 : 07:01 - 15:16 16/11 : 18:05 - 19:55
UPC, Barcelona Spain		1064	09/10/00 8:00 - 18:00 16/10/00 7:30 - 17:30
IMAAA, Potenza Italy	Day and night measurements since May. Some during all day.		ftp site
INFM, Napoli Italy	May to July and till September Some during all day.	1064,532, 351, 382	ftp site
LPAS, Lausanne Switzerland	No PBL observations because of high altitude	355, 532, 1064, 387	
ON, Neuchatel Switzerland	Full overlap above PBL top	532, 355	21/07 : 07.20 - 24.00 22/07 : 00.00 - 22.20 31/07 : 07.10 - 22.20
MIM, Munich Germany	Regular measurements only. No allday measurements this year.	ftp site	

Table 3.4: Summary of diurnal cycle observations.

Additional measurements are required for the analysis. Namely, radio-sonde measurements of pressure, temperature, moisture and wind speed at least twice a day (evolution forecast), lidar and aerosol optical thickness direct measurements (sun-photometers) for control. Measurements of radiation fluxes at the surface and chemical species are also to be considered.

In this first year of the EARLINET programme, the focus has been set on the methods of acquisition of known quality lidar data from all stations. As all the station did not have the same experience in lidar, consolidation of system operation and analysis methods were prioritised as compared to scientific analysis to get quality measurements and compare results. This is necessary to successfully analyse data, and not misinterpret the obtained results.

Different groups have started temporal cycle observations (France, Germany, Greece, Italy, Spain, Switzerland), mostly from time series with backscatter lidars and the data have been sent to the database at Max Planck Institute. The table 3.4 summarises the observations.

The strategy for the measurements needed within these WP has been discussed and consolidated



during the Athens workshop in March 2001. It was agreed to characterise structural parameters and optical properties of the boundary layer over a day.

Ideally, the objective is to make observations during the whole day starting before the sunrise and ending after sunset to observe the transition between the stable night-time and the unstable daytime boundary layer. As this represents a long observation period, and as processes involved are differently phased, it can be separated in the acquisition of several sets of observations for transitions in the morning and the evening, and observation of the maximum development of the PBL. Backscatter measurements during daytime will be reinforced by Raman measurements before and/or after sunset, whenever possible.

### **3.6.3 Socio-Economic relevance and policy implication**

The daytime evolution of the boundary layer is of importance as it may lead to reinforced pollution events when dynamical forcing prevents its development. The accumulation of aerosols and pollutants is thus increased, and specific actions may be necessary, such as limiting car traffic or industrial activity to avoid health damage on population.

It is very important to forecast these events due to their impact.

### **3.6.4 Discussion and conclusion**

Some data sets have up to now been obtained in the frame of at several stations during summer. Meteorological conditions have not been favourable in western Europe this autumn. In this first phase, observations were performed independently at different stations to check data quality and procedures.

### **3.6.5 Plan and Objectives for the next period**

Results and procedures have been discussed after this first year at the Athens workshop. It is the objective to move to more coordinated observations at the European scale during favourable meteorological situations. Measurements will be performed in prevailing high pressure conditions transitions to help several stations to observe transitions simultaneously. However measurements will be decided at the station operator level.

The objective is to make three measurement series (a series is a diurnal cycle observed during a day) per season (as for example during the summer season June-July-August) at all stations involved. Quasi-continuous measurements are aimed at for the retrieval of the structural parameters. The time interval between profiles should be shorter than during the regular measurements (typically five minutes). However a few sequences of twenty minutes including profiles every minutes are acceptable. Specific files will be made, and identified in a dedicated list in the ftp site. For the retrieval of optical parameters, measurements of the extinction coefficient are to be made at sunrise and/or sunset using Raman lidars. Backscatter coefficient is to be retrieved during daytime from backscatter measurements.

## 3.7 WP7, Observation of special events

by Alexandros Papayannis

### 3.7.1 Objectives

The main objectives of WP7 are focused on the implementation of a routine monitoring scheme, mainly in the South-European region for the observation of specifically high aerosol loads in the lower troposphere, resulting from extreme dust events (transport of Saharan dust, break of forest/industrial fires, intense photochemical smog episodes, etc.).

### 3.7.2 Methodology

To achieve the objectives eight of the EARLINET lidar stations located in the Southern Europe (Portugal, Spain, France, Italy and Greece) have been selected to perform extra lidar soundings under conditions of particularly high aerosol loads. The measurement frequency was initially set to 6-8 events/year, with 4-6 h measurements per event. Additional lidar stations were also selected in Central and Northern European sites (Switzerland, Germany, Poland, Belarus), to investigate on the long-range transport of Saharan dust aerosols across the European continent.

The coordination of the special lidar measurements was performed by the NTUA group, using forecasted Saharan dust events data available on the World Wide Web:

*<http://forecast.uoa.gr>*

validation data from satellite measurements

Aerosol Optical Thickness data (NOAA/AVHRR):

*<http://psbsgi1.nesdis.noaa.gov:8080/PSB/EPS/Aerosol/data/aerday.html>*

Aerosol Index data:

*[http://jwocky.gsfc.nasa.gov/from the TOMS instrument](http://jwocky.gsfc.nasa.gov/from_the_TOMS_instrument)*

Visible Images of Saharan dust storms from the SeaWIFS instrument:

*<http://seawifs.gsfc.nasa.gov/SEAWIFS/IMAGES/IMAGES.html>*

Meteorological Observations from METEOSAT satellite:

*<http://www.wetterzentrale.de>*

meteorological forecast data from ECMWF/UK:

*<http://grads.iges.org/pix/euro.fcst.html>*

and historic meteorological analysis data from Infomet, Spain:

*<http://www.infomet.fcr.es/arxiu>*

Ancillary measurements included routine observations of the aerosol optical depth at several UV/VIS/IR wavelengths using automated sun-tracking photometers and spectral UV radiance measurements, at selected EARLINET sites (IPSL/France, INFM/Italy, AUTH/Greece).

### 3.7.3 Scientific achievements

**Saharan dust events** The NTUA group, right from the start of the lidar measurements, on May 1, 2000, was in charge of the emission of special warnings, forecasting the time the Saharan dust events would overpass the respective EARLINET lidar sites. Table WP7-1, presents a summary of the Saharan dust events occurred during the 1st reporting period. In total, more than 13 Saharan dust episodes (each ranging from 1 to 5 days) were successfully forecasted by NTUA, and were subsequently identified and observed by the EARLINET stations, as will be detailed in the next

date/station	at	ba	be	gp	ju	la	lc	mi	na	ne	pl	po	th
08.–12.05.00	x	x				x	x		x	x		x	
15. – 18.05.00		x				x							
24. – 25.05.00					x								
27. – 29.05.00							x			x	x	x	
06.07.00	x												
<b>23. – 27.07.00</b>	x	x					x					x	
21.08.00				x									
<b>28.08. – 01.09.00</b>	x				x		x					x	x
11.–25.09.00	x			x		x	x				x	x	
<b>01.–05.10.00</b>	x		x					x					x
<b>12.–14.10.00</b>	x	x		x		x	x		x			x	x
31.10.00				x									
13.11.00	x												
16.11.00	x												
<b>30.01.–06.02.01</b>	x			x	x			x			x		

Table 3.5: List of Saharan dust episodes in the Mediterranean Region and Central Europe within the period 01.05.00 – 31.01.01. Bold dates correspond to major Saharan dust events (aerosol index a.i. > 1.8).

paragraph. Bold dates (5 cases) correspond to major Saharan dust events (Aerosol Index  $\geq$  1.8 in the 0.3-2.3 scale of the TOMS instrument).

Special attention should be paid to the following three special cases:

**CASE I** This was a case lasting as long as five days (08-12.05.00) which was successfully followed by 7 lidar stations in South/Southeastern, Central and Western Europe (see Table WP7-1). In this successful case distinct Saharan dust layers were observed in the height region from 2.5 km up to 5 km ASL (over the Mediterranean area), while they reached heights between 3-6 km ASL, when they overpassed Central Europe.

**CASE II** This case again lasting as long as five days (01-05.10.00), was successfully followed by 3 lidar stations in Southeastern and Eastern Europe (see Table WP7-1). In this case distinct Saharan dust layers were observed in the height region from 2.5 km up to 5.5 km ASL (over the Mediterranean area), while they reached heights between 3-7 km ASL when they overpassed Eastern Europe (Poland, Belarus). This is the first case of a Saharan dust event to be detected by lidars, both in the Southeastern (Greece) and Eastern (Poland, Belarus) Europe.

**CASE III** Case III lasted for three days (12-14.10.00) and was successfully followed by 7 lidar stations in South/Southeastern, Central and Western Europe (see Table WP7-1). Several distinct Saharan dust layers were observed in the height region from 2.5 km up to 5 km ASL (over the Mediterranean area), while they reached heights between 3.5-7 km ASL, when they overpassed Central (Alps region) and Western Europe (France).

Figure WP7-1 presents some selected altitude-resolved lidar profiles, where distinct layers of Saharan dust are clearly seen (cases I, II, III).

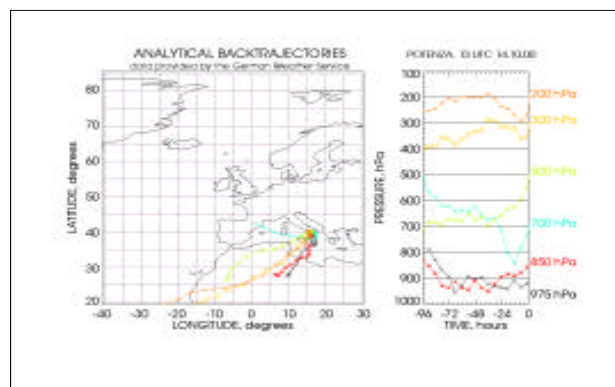
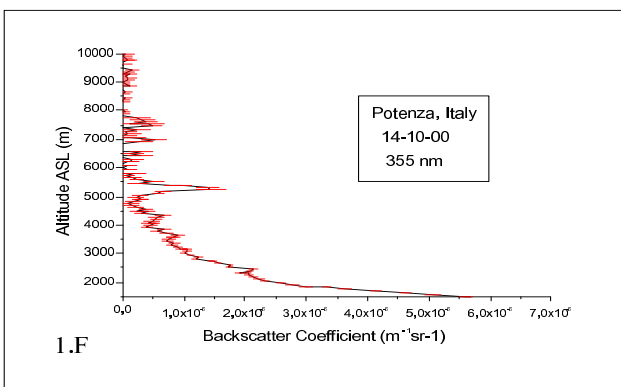
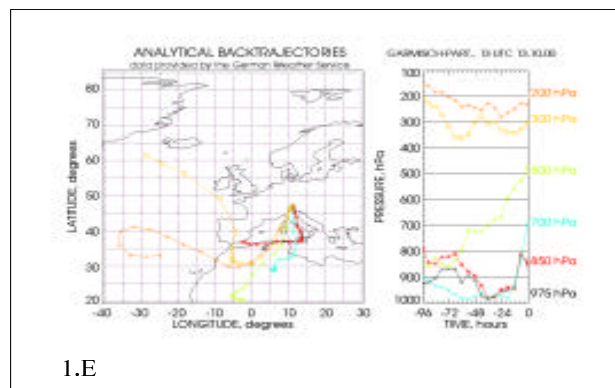
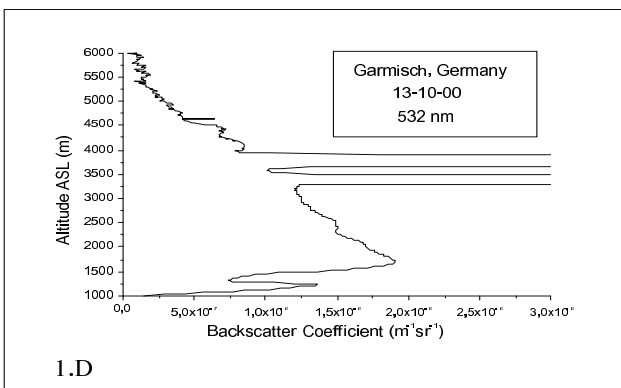
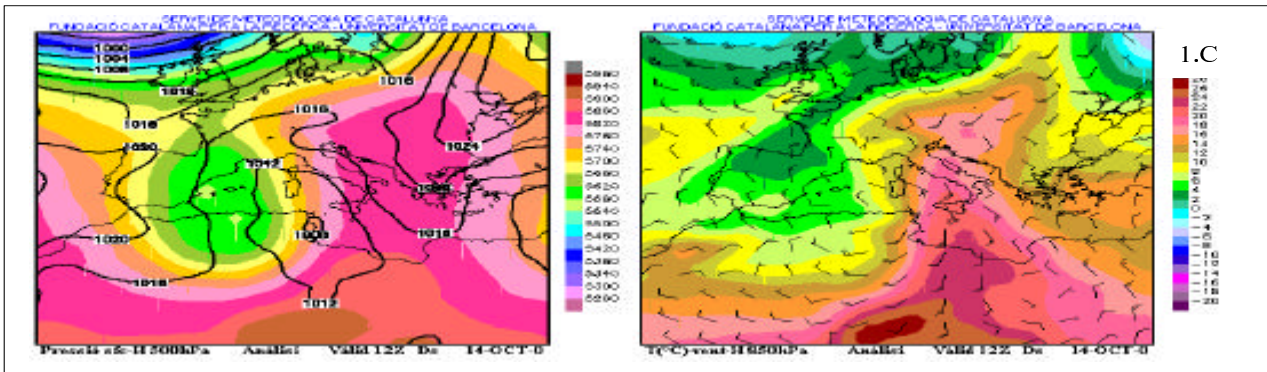
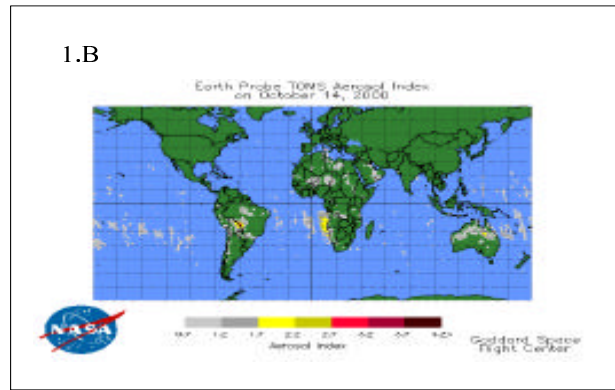
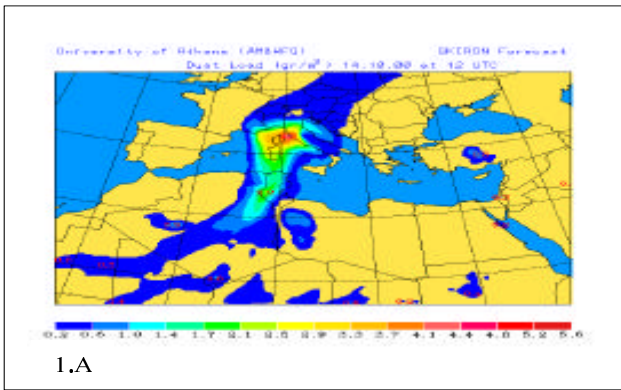


**Figure WP7-1:** Three days (12-14/10/00) Saharan dust episode: 1A: Dust event forecast from University of Athens (14/10/00, 12:00 UT), 1B: TOMS Aerosol Index data (14/10/00). 1C: Meteorological analysis from University of Barcelona (14/10/00, 12:00 UT). 1D,1F: Aerosol Backscatter lidar data obtained over Garmisch., Germany (13/10/00) and over Potenza, Italy (14/10/00), respectively, with respective (1E, 1G) backward air-mass trajectories.

In support to the lidar observations, backward air-mass trajectory analysis was performed (see WP4) by the German Weather Service (DWD), valid for each lidar station every day at 13:00 UT and 19:00 UT. In the case of the detected Saharan dust layers, all backward trajectory data (2-4 days earlier) had as origin the Saharan region (Fig. WP7-1). Additionally, the day-to-day analysis of the available meteorological and satellite observations (i.e. TOMS aerosol index, NOAA aerosol optical thickness, SeaWifs images) verified the lidar observations and confirmed the horizontal extent of Saharan dust events over Europe (Fig. WP7-1).

These observations enabled the establishment of the largest data set on simultaneous lidar observations, available so far, following the horizontal and vertical distribution of free tropospheric Saharan dust layers over Europe. As a conclusion, the prevailing synoptic meteorological conditions, from spring to autumn 2000 in the Mediterranean Sea, were proved to be very favourable in the long-range transport of large Saharan dust quantities from Africa up to Western, Central and Eastern Europe.

**Forest fires** In addition, during the same reporting period, plumes from several forest fires were observed by the lidar systems, 2 over the city of Athens on 26.06.00 and 13.07.00 (NTUA/Greece), 1 over the city of Barcelona on 06-07.08.00 (UPC/Spain) and 1 over the city of Aberystwyth on 11.08.00 (UABER/UK), through long-range transport from USA. In the case of the plume over Athens the largest aerosols concentrations were observed over the top of the Atmospheric Boundary Layer (ABL) around 2.2 km ASL, as well as at higher altitudes in the free troposphere (3-3.5 km ASL).

**Photochemical smog episodes** Regarding photochemical smog episodes, 5 important cases (26.06, 06.07, 27.07, 28.08 and on 13-22.09.00) were monitored by the NTUA's lidar group in Athens, Greece. In all cases the aerosol backscatter coefficients observed at 532 nm, overpassed the mean values (0.005-0.01 km<sup>-1</sup>sr<sup>-1</sup>) valid for the city of Athens, by a factor at least 1.5 to 3. In all cases, the highest aerosol concentrations were observed between 1.5-2.0 km ASL, around 13:00-14:00 UT, while the ABL height reached maximum values of 2.5-3 km ASL (spring/summer seasons) and 2-2.5 km ASL (autumn season) around 13:00 UT.

### **3.7.4 Socio-economic relevance and policy implication**

The main direct product of WP7, during its first year of operation, is a data set on the vertical, horizontal and temporal distribution of aerosols, occurred during special events (Saharan dust outbreaks, forest/industrial fires, photochemical smog episodes) over Europe. This is the first data set on a continental scale, therefore there is significant interest in the science community to use these data, for the improvement of global/regional atmospheric or of climate prediction models. Scientific publications and conference presentations, resulting from WP7, will give the opportunity to the science community to address the mechanisms of local aerosol formation, to study the trans-boundary transport processes of air pollution over Europe and to study the impact of aerosol loads in the earth's radiation budget and their link to Global Change. Finally, the necessary measures could be proposed for an air pollution abatement strategy in Europe, in compliance with the EU air pollution abatement/Climate Change policy.

### **3.7.5 Discussion and conclusion**

Important activities, in full accordance with the contract, were implemented right from the start of the project. The NTUA group organized the forecast procedure regarding the Saharan dust events over

Europe. In total, more than 13 Saharan dust episodes were successfully forecasted by NTUA, and were identified and observed by various lidar stations around Europe. These observations enabled the establishment of the largest data set, available so far, on simultaneous lidar observations, regarding the horizontal and vertical (altitude-resolved) distribution of free tropospheric Saharan dust layers over Europe. The prevailing synoptic meteorological conditions, from spring to autumn 2000 in the Mediterranean Sea, were proved to be very favourable in the long-range transport of large Saharan dust quantities from Africa up to the Central, North and even up to the Eastern Europe. In support to the lidar observations, backward air-mass trajectory analysis, as well as meteorological and satellite observations were analysed and strongly supported our observations and our conclusions. In addition, during the same reporting period, several plumes from forest fires were observed by the lidar systems, 2 over the city of Athens (NTUA/Greece), 1 over the city of Barcelona (UPC/Spain) and 1 over the city of Aberystwyth (UABER/UK), through long-range transport from USA. Regarding photochemical smog episodes, 5 important episodes (in spring/summer/autumn) were monitored by NTUA's lidar group in Athens, Greece.

### **3.7.6 Plan and objectives for the next period**

The detailed plan and objectives for the year 2001, include the same forecasting and monitoring scheme, in view to maximize, not only the number of events observed, but also the monitoring period, to get a more detailed follow-up of the diurnal variation of the horizontal and vertical extent of the aerosols distribution over Europe, during the occurrence of important Saharan dust events. Data analysis from routine observations of the aerosol optical depth at several UV/VIS/IR wavelengths, using automated sun-tracking photometers and spectral UV radiance measurements, at selected EARLINET sites (IPSL/France, INFM/Italy, AUTH/Greece) will be performed during 2001. The scientific material collected so far, for all three subsets (Saharan dust events, photochemical smog episodes, forest/industrial fires), forms already a very solid basis for relevant detailed studies of the associated meteorological and photochemical processes over Europe. The output of WP7 could be directly used for the quantification of the Saharan dust transported from Africa to the European continent.

## 3.8 WP8, Impact on satellite retrievals

by Matthias Wiegner

Workpackage 8 provides a link between active remote sensing by lidars (EARLINET) and passive remote sensing by satellite-borne radiometers. In particular with respect to aerosols, the potential of radiometers is quite limited: while the monitoring of the aerosol optical depth over oceans shows some encouraging results, the retrieval of aerosol properties over land surfaces is – in principle – difficult and still in the stage of testing. As a consequence, datasets for validation are desperately required. Lidar measurements from EARLINET are certainly a natural candidate for doing so, in spite of their limited spatial and temporal coverage. Thus, two approaches are possible: first, the provision of special lidar measurements to validate co-incident and co-located satellite measurements, and second, the provision of local climatologies and annual cycles that can be compared to respective quantities derived from satellites.

A second topic of this workpackage includes the modeling of the aerosol influence on radiances as measured by satellites. Such model calculations – with realistic aerosol profiles gained from the EARLINET measurements – can help to assess the radiative forcing of aerosols, corrections for atmospheric masking, the required sensitivity and accuracy of satellite-borne instruments, and typical spatial and temporal scales adequate for averaging. In particular the last point is of interest because the spatial resolution from space is often quite poor.

These topics are very ambitious. Therefore, it is necessary to restrict ourselves to the investigation of few examples, and we must rely on support from the satellite community. In accordance to the milestone plan, lidar measurements are provided since May 2000. First dedicated measurements simultaneous to satellite overpasses are scheduled for the second half of 2001 in the frame of PROBA/CHRIS validation campaigns, where lidar measurements near Munich were accepted as a core site. The detailing of the measurement scenario will start soon. In addition, first contacts to scientists working on the development of algorithms for aerosol detection over land have been launched. At the present stage, the contribution of both sides and the exchange of data is discussed. As already stated, the provision of climatological datasets certainly will also be valuable for satellite retrievals. This benefit will mainly be visible at the end of the project.

The model calculation activities started in Month 6 of EARLINET by reviewing the available radiative transfer codes. Several calculations of shortwave radiances at the top of the atmosphere for different aerosol types and distributions have meanwhile been performed. They confirm the inherent difficulties of passive remote sensing techniques for aerosol detection.

### 3.9 WP9, Air mass modification processes

by Ulla Wandinger

The distribution of the lidar-network stations in Europe gives the opportunity to study the anthropogenic influence on the aerosol. Clean (pristine) air arriving from maritime and polar regions is detected by the most northerly and westerly stations (Linköping, Aberystwyth, Hamburg). Traveling across Europe, these air masses are modified according to anthropogenic activities, by which precursor gases and particles are emitted into the atmosphere. Depending on travel distance and residence time over the source regions, particle number concentrations, the physical and chemical state and thus the optical properties of the aerosol change. The comparison of particle backscatter and extinction profiles measured at the stations in central and eastern Europe with those at the boundaries of the network will permit us to quantify the anthropogenic impact. Figure 3.13 illustrates the idea of this study. The investigations will be limited to the northern part of the network, where orographic effects on aerosol modification processes are of minor importance.

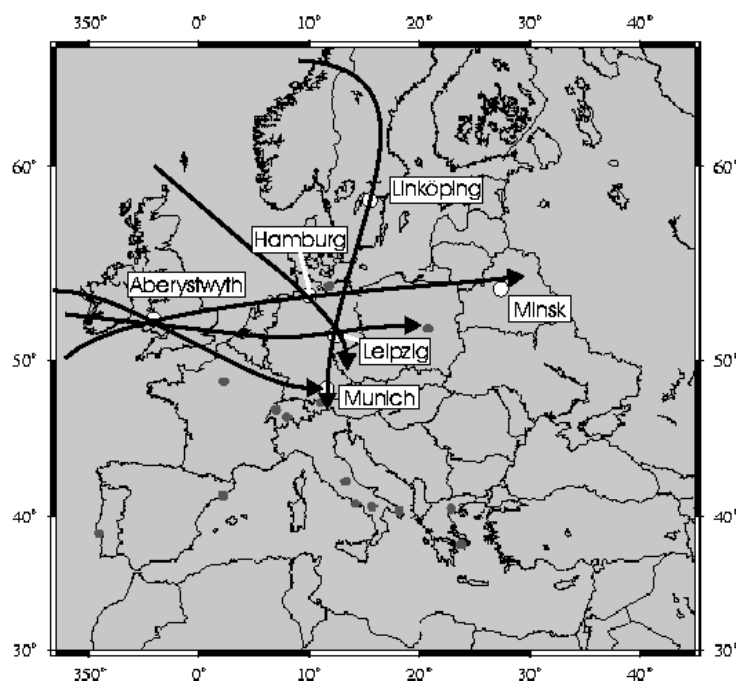


Figure 3.13: Typical advection schemes for marine and polar air masses over Europe.

Two strategies have been suggested for the activities of this workpackage. First, coordinated measurements based on prognostic forward trajectories should be performed. A detailed look into the modification processes is possible on the basis of the resulting sample of case studies. However, the typical travel times of air parcels from the remote stations (Aberystwyth, Linköping; clean marine conditions) to central and eastern Europe (Leipzig, Munich, Minsk; polluted conditions) are of the



order of two to four days. The trajectory data base for the first six months of experimental work shows that in many cases the prognostic trajectories did not adequately forecast the actual transport of air for such long travel times and distances. Thus, coordinated activities are hard to realize and will be limited to few examples.

Therefore, it was decided to concentrate the activities of this workpackage on a statistical approach. Based on the routine, long-term measurements at the different stations (data from WP2) and an appropriate analysis of analytical backward trajectories (data from WP4), the increase of the aerosol load in air masses that cross Europe from west to east or from north to south can be quantified. For the remote stations, typical profiles for air masses reaching Europe from the Atlantic will be determined, e.g., in dependence on the season. These profiles will be compared with those taken in central and eastern Europe under conditions, for which the air masses traveled from the Atlantic across well-defined European regions to the measurement sites. Trajectory analysis will help to classify the measurements. A cluster-analysis software developed at IfT will be used for this purpose. First investigations for the German network stations based on a three-year data set of backward trajectories showed that all of these central-European sites are influenced by similar advection schemes. Three of five trajectory classes indicate conditions, for which the air masses come either from the Atlantic across western Europe or from the North Sea and Scandinavia to Germany. The statistical approach will thus be based on a very large data set and will deliver statistically significant data.

## **3.10 WP10, Orography and vertical transport**

by Thomas Trickl

### **3.10.1 Objectives**

The main objective is to study air pollution export from the boundary layer promoted by mountains under the rather different conditions of the individual partner stations. It is desirable to obtain material on the interaction with the synoptic wind and on how the boundary-layer air is injected to the free troposphere.

### **3.10.2 Methods**

The aerosol backscatter coefficient, under conditions of low to moderate humidity, is an excellent tracer for air-mass exchange. The transport processes are followed by diurnal series of lidar soundings. Information on the wind field is crucial for an interpretation of the data. This information may be provided by radio-sonde ascents or aircraft flights.

### **3.10.3 Scientific achievements**

In 2000, three stations (Athens (AT), Barcelona (BA), Garmisch-Partenkirchen (GP) have been active for WP10. The results are, still, sparse.

An example for convective transport in the mountainous area of Athens is depicted in Fig. 3.10.3. The aerosol is transported to altitudes of 5 km a.s.l. and drifts through the slant-path laser beam (directed over a 1.5 km high mountain) in the orographic wind building up between the coastal area and the sea. The wind direction from the city to the sea aloft was verified by models and the 12 UT radiosonde for that day.

At IFU, just a limited number of lidar measurements were made due the ongoing reconstruction mainly caused by problems with the IR detection electronics. The measurements are restricted to 532 nm. No new interesting cases for the vertical transport in the local orographic wind systems were detected. A field campaign including the ultralight aeroplane of the institute had been planned for August 2000 after installing and successfully testing wind sensors onboard the aircraft. Eventually, the campaign had to be cancelled. The next attempt will be made in spring 2001.

The cases studied within the German Lidar Network have been analysed during the reporting period. It turns out that a valley-wind–anti-valley-wind circulation may form under conditions of low synoptic wind speed aloft. A counter example was found in spring (April 7, 2000): In the presence of strong northerly winds towards the Alps no aerosol was seen at all above the boundary layer which indicates a strong interference by the wind.

### **3.10.4 Socio-economic relevance and policy implications**

The air-pollution export from the boundary layer to the free troposphere is crucial for the hemispherical distribution of pollutants. Significant amounts of trace gases such as ozone, but also some aerosol are transported from continent to continent. This should have severe implications for the most productive source regions for air pollution such as South-East Asia, North America and Europe.

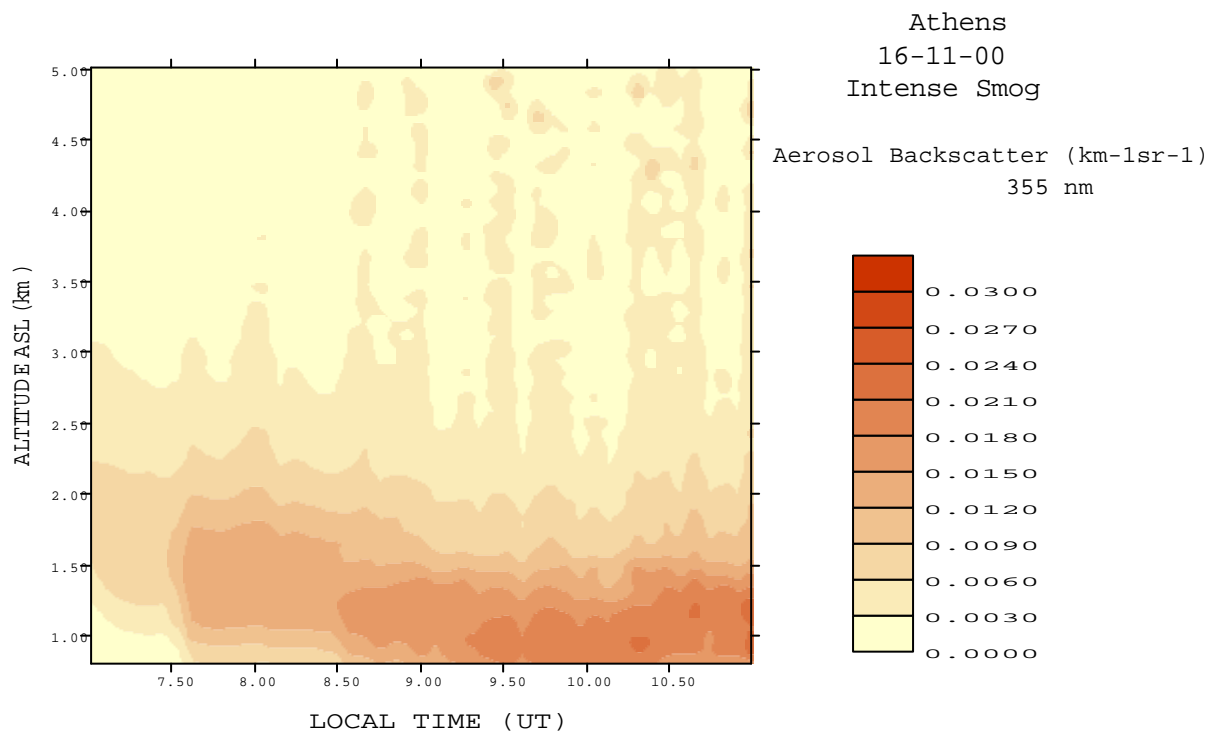


Figure 1: Evolution of the aerosol backscatter coefficient Baer at 355 nm over the city of Athens (161100). This is an example of intense photochemical smog in conjunction with increased relative humidity. Rising plumes due to thermal convection are clearly seen, while the sea-breeze circulation over Athens is observed around 9:00-9:30 UT, where enhanced Baer values are observed due to the transport of polluted air masses over the lidar site, originating from downtown of the city of Athens.

### 3.10.5 Discussion and conclusion

A full discussion is not yet possible at this stage of the project.

### 3.10.6 Plan and objectives for the next period

Intensified efforts will be made at IFU. At least two field campaigns including aircraft measurements are planned. At the other stations the case studies will be continued.

## 3.11 WP11, Stratospheric aerosol

by Bertrand Calpini

The first objective of WP11 is to coordinate stratospheric aerosol observation by lidar over Europe. A subgroup of 6 partners operating the stations at Aberystwyth, Leipzig, Kühlungsborn, Napoli, L'Aquila, and Jungfraujoch is active in this area. Since some months the lidar team from the National Academy of Sciences of Belarus in Minsk is also a member of this community.

In this coordination of WP11, EPFL is also in charge of the announcement (warning) for special period of observations. In particular, alerts for volcano eruption were followed on a day by day basis, especially for the case of some recent eruptions events at the Popocatepl. None of these eruptions did ever reach the different Earlinet sites, or at least were not detected within the network. We have to point out here that year 2000 was characterized by very low aerosol activity at high altitude in the free troposphere or low stratosphere. Lidar observations at high altitude were also perturbed for very long period of time due to important cloud covering and a rather poor meteorological conditions, especially during late 2000.

The second task within WP11 is the detection of small scale feature in the aerosol distribution in the lower stratosphere. Two special events were reported during this first reporting period, both by the Kühlungsborn group : Between September 18 and 25, 2000 an aerosol layer between 14 and 17 km was observed and also reported at L'Aquila, Kühlungsborn, and Minsk while the other stations were again "cloud covered". On November 22, 2000 an aerosol layer at an altitude of 37 km was observed measured in Norway at the ALOMAR station (69N). While such altitude range is generally unlikely to happen, this observation was reported for a period of time, with a rather fine but well defined structure and a vertical extension of only 1 km. It reached a maximum backscatter ratio of 1.4 (1064 nm). Unfortunately at the same period, all the other Earlinet stratospheric stations were under dense clouds conditions.

## **3.12 WP12, Differences rural-urban aerosols**

by Jacques Pelon

### **3.12.1 Objectives**

The objective of the work to be performed in this WP is close to the one of WP6, as focusing on the difference between urban and rural aerosols which can be observed during temporal cycles. The diurnal and seasonal cycle of the aerosols in the boundary layer is different over urbanised and agricultural surfaces as solar forcing and dynamical production will be different at the surface. A heat island is formed in urban areas, which modifies circulation, and transport of aerosols at the meso-scale. Furthermore, important sources of pollution are present in or near cities as traffic is more important as well as industrial activity. This impacts the optical parameters of the aerosol layers, which are different in urban and rural areas.

### **3.12.2 Methodology and scientific achievements**

Five pairs of groups are involved in this work. Methodology is similar to WP6 and implies to observe the transition between the stable nighttime and the more convective daytime boundary layer, aiming at the acquisition of two sets one for the morning and the other for the evening transitions, as the behaviour of the urban boundary layer is different than the rural one. This is due to both an increase in roughness at the surface due to the buildings elevation, and to the anthropic heat flux caused by heat accumulation during daytime and manmade production in urban areas. The development of the boundary layer will thus be different in town and outside and the optical properties may differ as well.

Additional measurements similar to WP6 are also required for the analysis.

The same remarks as for WP6 apply to WP12 for the data acquisition and analysis. First cases have been observed, but priority was given to setting the network and ensuring data quality.

## 3.13 WP13, UV-B and optical properties

by Dimitris Balis

### 3.13.1 Objectives

The main objectives of WP13 are:

- To perform UV-B radiation measurements simultaneously with the lidar measurements
- To validate the radiative transfer models against UV-B measurements, using additional the lidar as input to the model calculations.
- To estimate the impact of different aerosol conditions on the UV-B radiation field, using both measurements and model calculations

### 3.13.2 Methodology and scientific achievements

At the Thessaloniki station two UV spectrophotometers (one single and one double monochromator) operate continuously and monitor, with a 0.5 nm spectral resolution, the whole UV solar spectrum. In addition measurements of global total, UV-A and UV-B radiation, direct and diffuse erythematous irradiance are being performed. In addition a program for monitoring the O<sub>3</sub> and SO<sub>2</sub> total columns is in operation, which will be used as input to the model. At Athens measurements of the global UV erythematous irradiance are available. At Garmisch-Partenkirchen spectral UV measurements are performed.

During the first year of EARLINET, the Tropospheric Ultraviolet and Visible (TUV) Version 4 model was tested against spectral UV-B measurements and its accuracy was found to be better than 10% when the input parameters were well defined. The model is available through anonymous ftp, by Dr. Sasha Madronich (National Centre of Atmospheric Research). In order to solve the radiative transfer equation, we are using the discrete-ordinates algorithm (DISORT) developed by Stamnes et al. (1988), using 16 streams. This routine is also used by other state of the art radiative transfer codes (e.g. UVSPEC). In TUV the atmosphere is divided in 50 adjacent and homogeneous layers. In each of them it is assumed that scattering and absorbing properties are constant, but are allowed to be different from layer to layer. The comparisons of model results and direct radiation measurements show rather good agreement, clearly better than 10% with few exceptions (Figure 3.14).

### 3.13.3 Discussion and conclusion

From the lidar measurements performed at urban sites of Thessaloniki and Athens certain cases have been identified with variable conditions concerning the vertical distribution of aerosols and the total ozone amount. These cases are listed in Table 3.6, along with the available UV-B measurements. The UV-B erythematous irradiance measurements in Thessaloniki and Athens have been calibrated, while the spectral UV-B measurements are pending final calibration. UV-B measurements from IFU are still under evaluation.

In figure 3.15 we present a case study with the same total ozone content and variable aerosol conditions over Thessaloniki. As it obvious from this case the ratio of the UV erythematous irradiance is attenuated by almost 10% from the Sahara dust layer, depending on the solar zenith angle, compared

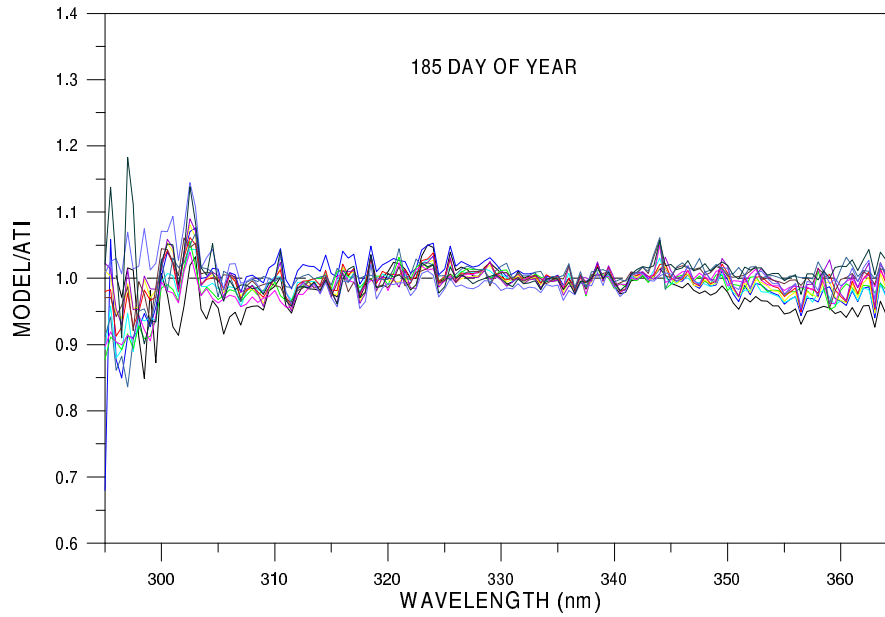


Figure 3.14: Diurnal variation of the ratio between calculated solar irradiance, averaged over the 5nm region centered at 340nm, to that measured by the double monochromator. Different values of the single-scattering albedo ( $\omega$ ) were used in the model calculations, and the corresponding ratios are represented by different colors. This suggests that different values of  $\omega$  should be used for each spectrum to make the ratio equal to unity.

Table 3.6:

Date	Location	Ozone(D.U.)	Aerosol remarks
21/06/2000	Athens	314	Sahara dust episode
06/07/2000	Athens	291	Sahara dust episode
27/07/2000	Athens	300	Sahara dust episode
28/08/2000	Athens	289	Sahara dust episode
14/08/2000	Thessaloniki	305	Clean aerosol conditions
31/08/2000	Thessaloniki	305	Sahara dust episode
14/09/2000	Athens	302	Sahara dust episode
18/09/2000	Athens	305	Sahara dust episode
21/09/2000	Athens	274	Sahara dust episode
25/09/2000	Thessaloniki	288	Clean aerosol conditions
02/10/2000	Thessaloniki	263	Sahara dust episode
12/10/2000	Thessaloniki	290	Sahara dust episode

to the case with no Sahara dust. The ratio of the shortwave irradiance is also attenuated by as much as 30%.

In figure 3.16 we present the corresponding height profiles of the aerosol extinction coefficients for the two days:

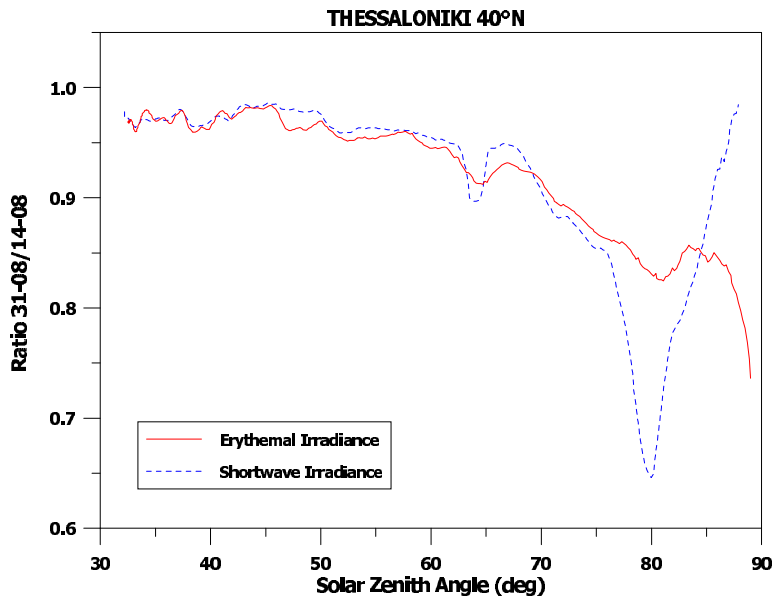


Figure 3.15: Ratio of UV-erythema irradiance for a Sahara dust episode (31-08) and for a regular aerosol situation (14-08) (red line) and the corresponding ratio of shortwave irradiance (blue-dashed line).

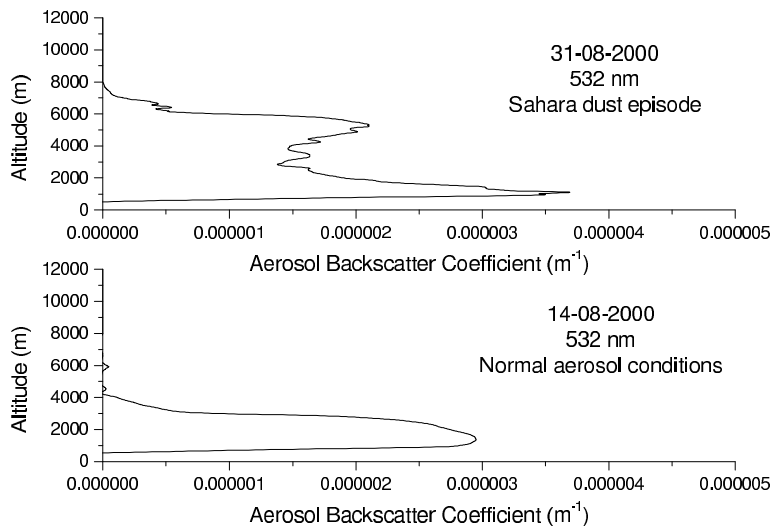


Figure 3.16: Aerosol backscatter coefficient ( $\text{m}^{-1}\text{sr}^{-1}$ ) for the Sahara dust episode and for a day with “normal” aerosol conditions.

### 3.13.4 Plan and objectives for the next period

Further improvements to model calculations, regarding the accuracy of the aerosol extinction profiles derived by lidar measurements, are ongoing. The first improvement is already done, by the most accurate calculation of the extinction profiles from N2 Raman lidar signals. The other great source of uncertainty in model calculations is the estimation of the single-scattering albedo ( $\bar{\omega}$ ) and the asymmetry factor ( $g$ ). Both  $\bar{\omega}$  and  $g$  depend on wavelength, on the size and the chemical composition of the aerosols, as well as on the relative humidity. For different types of aerosols, typical for the



atmospheric boundary layer,  $\omega$  and  $g$  in the UV are expected to vary respectively from 0.65 to 0.99 and from 0.5 to 0.9 (van der Hulst, 1957; Shettle and Fenn, 1979). Sensitivity studies (Kylling et al., 1998) have shown that, compared to the asymmetry factor, the single-scattering albedo is more effective in modifying the UV irradiance, because it alters significantly its diffuse part. The accuracy of the model's calculations will be improved, by estimating the height profile of the lidar ratio. This will be accomplished by the calculation of particle backscatter coefficient from the combination of one lidar equation for the elastic backscatter signal (355 nm) and one Raman lidar equation (387 nm). Routine measurements according to EARLINET's schedule will be performed, measurements during special events and UV-B measurements. The main objective for the next period will be the comparison of the TUV model's calculations with the UV measurements (spectral and broadband) for the cases that the model inputs are well defined. These comparisons will help to quantify the influence of different aerosol types and variable aerosol load on the UV-spectrum. This analysis will be presented at the EAC in Leipzig, 2001, and a journal paper will be prepared.

### **3.14 WP14, Statistical analysis**

**by Jens Bösenberg**

In accordance with the statement of work the activities regarding this work package have not yet been started.

## **3.15 WP15, Lidar ratio data base**

by Gelsomina Pappalardo

### **3.15.1 Objectives**

The main objective of WP15 is the compilation of a statistically significant data set concerning the ratio of aerosol extinction to backscatter (lidar ratio) starting from both regular and special measurements. These measurements will cover a broad range of meteorological conditions, and in conjunction with information on the air mass characteristics can give information on microphysical properties of the aerosols.

### **3.15.2 Methodology and scientific achievements**

To achieve the objectives of this WP, all the EARLINET lidar stations providing simultaneous aerosol extinction and backscatter measurements have been selected. Nine lidar stations have the capability of measuring nitrogen Raman scattering in the UV simultaneously to the elastic backscatter; among these lidar stations two have the capability to measure nitrogen Raman scattering also in the visible (Kühlungsborn and Leipzig). Seven lidar stations have a scanning capability and hence their data can be used to retrieve the aerosol extinction profile. Within the EARLINET community a big effort has been devoted to upgrade the Raman capability and an increasing number of stations is going to be equipped with Raman channels. A working group about determination of aerosol extinction profiles from Raman measurements has been installed. This group supplied guidelines for the evaluation of Raman signals to the EARLINET community. A training case with simulated Raman signals, with known solution, was made available for all groups to test their own algorithms.

### **3.15.3 Socio-economic relevance and policy implication**

The main direct product of WP15, during its first year of operation, is a data set on the lidar ratio values obtained in a significant number of stations in Europe. This is the first data set on a continental scale, therefore there will be significant interest in the scientific community to use these data for the improvement of both global/regional atmospheric and climate prediction models. Moreover, these data will be important for aerosols studies performed by future space based lidar (PICASSO-CENA, ELISE, ERM).

### **3.15.4 Discussion and conclusion**

Data provided by the groups performing simultaneous aerosol extinction and backscatter measurements have been collected in order to start the compilation of a statistically significant data set concerning the ratio of aerosol extinction to backscatter (lidar ratio). Data have been divided into regular and special measurements. Regular measurements can provide a significant data set of lidar ratio values obtained over a broad range of meteorological conditions on a continental scale. Special measurements can provide a data set of values of the lidar ratio during special events (Saharan dust outbreaks, forest/industrial fires, photochemical smog episodes) over Europe. Both these data sets are important for investigating the aerosols impact on climate.

The aerosol extinction coefficient can be determined from the  $N_2$  (or  $O_2$ ) Raman backscattering signals through the application of the derivative of the logarithm of the ratio of the atmospheric number

density and the range corrected lidar-received power. This type of calculation is not straightforward since both aerosol extinction coefficient and its error can be miscalculated if data acquisition and analysis are not correctly accomplished. For this reason, big care is necessary in handling data in order to retrieve the extinction coefficient profile starting from Raman signals. The working group on the extinction retrieval supplied a document to the whole EARLINET community providing the guidelines for the evaluation of the aerosol extinction coefficient from Raman measurements. In such a document, a list of rules and suggestions to be followed, together with some useful references, has been given.

### **3.15.5 Plan and objectives for the next period**

A statistical analysis on the lidar ratio data set obtained during the first year of the project will be performed. When possible, the wavelength dependence will be studied both for regular and special measurements. Results will be combined with information on the air mass characteristics. Data provided by the groups performing simultaneous aerosol extinction and backscatter measurements will be collected continuously in order to increase the data set concerning the lidar ratio. To this purpose, it is important to note that an increasing number of stations is going to be equipped with Raman channels, so that more data will become available in the next future. Results obtained from the training case for the retrieval of the aerosol extinction coefficient starting from Raman signals will be collected. It is expected that all groups come up with similar performance although this may require subsequently adjustments for some groups.

## **3.16 WP16, Analysis of source regions**

by Thomas Trickl

### **3.16.1 Objectives**

Based on the aerosol soundings within the lidar network the importance of different long-range transport pathways will be determined. Focus is on extra-European aerosol sources such as the Sahara desert, the U.S.A. and wild fires in North America, in particular in the boreal regions of Canada. Since statistics for the Saharan dust events will be gathered in WP7 most effort will be on intercontinental transport.

### **3.16.2 Methods**

Aerosol signatures in the free troposphere are an excellent tracer for boundary-layer air. The importance of long-range transport from different source regions may be estimated from relating the cases with aerosol in the free troposphere to the total number of routine measurements. A more refined analysis will be based on distinguishing various classes of backward trajectories. The determination of relative fluxes can be attempted, but may be strongly biased due to elimination by processes such as washout in fronts.

### **3.16.3 Scientific achievements**

Contributions to WP16 have been received from Athens, Barcelona and Garmisch-Partenkirchen. The analysis of the cases submitted is in progress. A statistical analysis based on trajectories is expected from each of the contributing groups.

In 2000, a three-year statistical analysis (Sept. 1997 to Nov. 2000) of the free-tropospheric data obtained at Garmisch-Partenkirchen was made. Only data from layers clearly distinguishable from the aerosol-loaded lowermost troposphere have been used (thus, Saharan dust events are likely to be excluded from this study). A rather high fraction of cases with aerosol signatures was found, approximately 40%. A pronounced aerosol maximum exists in spring. More than 60% of the spring profiles showed distinguishable structures in the free troposphere. No trajectory analysis has so far been made, but will be done with the quickly growing data set and also with historical data.

In addition, aerosol from the Montana wild fires were observed in August 1998. The air mass was traced back to the source with ten-day trajectories and TOMS satellite images.

The Saharan-dust cases are reported within the Section of WP7.

### **3.16.4 Socio-economic relevance and policy implications**

The importance of intercontinental transport has long been overlooked. Significant amounts of trace gases such as ozone, but also some aerosol are transported from continent to continent. This should have severe implications for the most productive source regions for air pollution such as South-East Asia, North America and Europe.

### **3.16.5 Discussion and conclusion**

A full discussion is not yet possible at this stage of the project.

### **3.16.6 Plan and objectives for the next period**

The work at some of the stations is under way. We expect some more input from other stations with lidar systems with sufficiently high sensitivity in the free troposphere.

## 3.17 WP17, Microphysical retrieval algorithms

by Christine Böckmann

### 3.17.1 Objectives

Several instruments of the EARLINET lidar network deliver information on particle extinction and backscatter coefficients at multiple wavelengths. This information can be used to invert physical particle properties such as particle size, number, surface-area, and volume concentration, as well as complex refractive index. However, the inversion problem in a mathematical sense is non-linear and ill-posed and its solution requires the application of appropriate mathematical regularization methods. Therefore, one part of the project is to develop, to improve and to investigate inversion algorithms for optical data sets, which are obtained with different lidar systems of the network.

The set of backscatter coefficients at 355, 532, and 1064 nm and of extinction coefficients at 355 and 532 nm is the standard output of an advanced aerosol Raman lidar based on a single Nd:YAG laser. The stationary systems at IAP Kühlungsborn and IfT Leipzig make use of this configuration in EARLINET and some other groups plan an upgrade of their instruments to this standard output.

The IfT Leipzig system has the possibility to deliver three backscatter coefficients, additionally.

The IBNANB Minsk is able to get between two- and four-frequency sounding results.

The main objectives of WP17 are focused on the development of suitable retrieval algorithms for various systems and on theoretical mathematical investigations concerning the complex refractive index, the shape of the aerosol particles and new regularization techniques.

### 3.17.2 Methodology

The mathematical model, which relates the optical and the physical particle parameters, consists of a Fredholm system of two integral equations of the first kind for the backscatter and extinction coefficients  $\beta^{Aer}$  and  $\alpha^{Aer}$ :

$$\beta^{Aer}(\lambda, z) = \int_{r_0}^{r_1} K_{\pi}(r, \lambda, m, s) n(r, z) dr = \int_{r_0}^{r_1} \pi r^2 Q_{\pi}(r, \lambda, m) n(r, z) dr, \quad (3.7)$$

$$\alpha^{Aer}(\lambda, z) = \int_{r_0}^{r_1} K_{ext}(r, \lambda, m, s) n(r, z) dr = \int_{r_0}^{r_1} \pi r^2 Q_{ext}(r, \lambda, m) n(r, z) dr, \quad (3.8)$$

where  $r$  denotes the particle radius,  $m$  is the complex refractive index,  $s$  is the shape of the particles,  $r_0$  and  $r_1$  represent suitable lower and upper limits, respectively, of realistic radii,  $\lambda$  is the wavelength,  $z$  is the height,  $n$  is the particle size distribution we are looking for,  $K_{\pi}$  is the backscatter and  $K_{ext}$  is the extinction kernel. The kernel functions reflect shape, size, and material composition of the particles.

The following formulas hold for extinction and backscatter efficiencies of homogeneous spheres:

$$Q_{\pi} = \frac{1}{k^2 r^2} \left| \sum_{n=1}^{\infty} (2n+1) (-1)^n (a_n - b_n) \right|^2, \quad Q_{ext} = \frac{2}{k^2 r^2} \sum_{n=1}^{\infty} (2n+1) \text{Re}(a_n + b_n), \quad (3.9)$$

where  $k$  is the wave number defined by  $k = 2\pi/\lambda$  and  $a_n$  and  $b_n$  are the coefficients which one can get from the boundary conditions for the tangential components of the waves. Now Eqs. (3.7) and

(3.8) are formulated into a more specific and more solid form:

$$\Gamma^{Aer}(\lambda, z) = \int_{r_0}^{r_1} K_{\pi/ext}^v(r, \lambda, m) v(r, z) dr = \int_{r_0}^{r_1} \frac{3}{4r} Q_{\pi/ext}(r, \lambda, m) v(r, z) dr, \quad (3.10)$$

where the  $v(r, z)$  term is the volume concentration distribution we are finally looking for.  $\Gamma^{Aer}$  stands for  $\beta^{Aer}$  and/or  $\alpha^{Aer}$ , respectively, depending on the measurement data. The determination of the particle volume distribution  $v$  from a small number of backscatter and extinction measurements is an inverse ill-posed problem and because the refractive index  $m$  in the kernels  $K_{\pi/ext}^v$  is an unknown, too, the problem is a highly nonlinear one, i.e., solutions are non-unique and highly oscillating without the introduction of appropriate mathematical tools such as discretization and regularization.

### 3.17.3 Scientific achievements

**Algorithm I (UPIM):** Based on mathematical knowledge, a special hybrid regularization technique was developed. This hybrid regularization technique is designed to work with different kind and number of optical data, i.e., experimental data obtained with different systems at various wavelengths can be evaluated. The algorithm does neither require any *a priori* information on the analytical shape of the investigated distribution function nor an initial guess of it. Even bimodal and multimodal distributions can be retrieved without any knowledge of the number of modes in advance. The first regularization step in this method is performed via discretization, in which the investigated distribution function is approximated with variable B-spline functions. The projection dimension (number of basis functions) and the order of the used B splines serve as regularization parameters. In the second step, regularization is controlled by the level of truncated singular-value decomposition performed during the solution process of the resulting linear equation system. In order to reduce the computer time, a collocation projection is used. The highly nonlinear problem of the complex refractive index as a second unknown is handled by introducing a grid of a wavelength- and size-independent mean complex refractive index and by enclosing the area of possible real/imaginary-part combinations through inversion and back-calculation of optical data. Inversion results are given in terms of volume distributions, effective particle radius, volume, surface-area, and number concentrations. In addition, the unknown refractive index can be captured.

**Algorithm II (IfT):** The IfT scheme uses a Tikhonov regularization with constraints to invert the eight optical data measured with the IfT multiwavelength lidar. The strength of regularization, which determines the degree of smoothness of the solution, is found from generalized cross-validation. The investigated volume concentration distribution is approximated with a discrete set of eight basis functions, which have the shape of B splines of the second order, i.e., linear polynomials. Fifty inversion windows of variable width are defined through variation of the lower and upper limits of the basis-function range from 0.01 to 0.2 and from 1 to 10  $\mu\text{m}$ , respectively. The basis functions are distributed logarithmically equidistant within the windows. The inversion is performed for every window and for refractive indices that vary from 1.33 to 1.8 in real and from 0 to 0.7 in imaginary part.

From the inversion solutions only those are selected, for which the back-calculated optical data agree with the original data within the limits of the measurement error. Mean and integral particle parameters, i.e., effective radius, volume, surface-area, and number concentrations, are calculated from

the selected solutions, and their mean values and standard deviations are presented as final inversion results. Furthermore, the single-scattering albedo is calculated from the volume concentration distribution and the complex refractive index as in the UPIM algorithm, too.

**Algorithm III (IBNANB):** Firstly, we have designed an iteration algorithm to solve the so called lidar ( or sounding) equation and created a respective computer code. The algorithm accounts for features in the measurement procedure by lidar stations at Minsk and Belsk, namely the lidar calibration procedure by a screen. Moreover, we are making observations in the stratosphere. Thus, we have reference points at the beginning of a sounded path and at high altitudes as well as the two sets of the points simultaneously. The processing code retrieves profiles with accounting for specified errors in the profile at the reference points. While processing the sounding data along short paths, the calibration by a screen has the crucial importance. At the same time, it is useful as an indicator of non-linearity and noise effects of the measuring channel while processing extended paths. By using a wavelength- and height-dependend lidar ratio, one can use the designed code to independently process sounding.

Secondly, we assume to use multi-dimensional regression relations as constraints with taking a small number of input parameters into account. The problem is to determine the optimal regressions for different experimental conditions. We use the multi-dimensional linear regression of the form

$$\alpha^{Aer}(\lambda_i, z) = \sum_j c_{ji}(\lambda_i) \beta^{Aer}(\lambda_j, z). \quad (3.11)$$

The absolute term in Eq.(5) is assumed to be zero to provide this relation being independent of aerosol concentration. A statistical ensemble of distribution functions  $n(r, z)$  characterizing the probabilistic spread of aerosol sizes during measurements is preliminary constructed to find coefficients  $c_{ji}(\lambda_i)$ . Coefficients  $c_{ji}(\lambda_i)$  are determined from the condition for the functional minimum

$$g = \overline{[\alpha^{Aer}(\lambda_i) - \sum_j c_{ji}(\lambda_i) \beta^{Aer}(\lambda_j)]^2} = \min, \quad (3.12)$$

where the bar denotes the averaging by some statistical ensemble of functions  $n(r, z)$ . A key issue to find coefficients is the selection of the statistical ensemble of functions that characterizes the size spread. A priori information on scatterers and independent measurements are used to restrict possible variations in  $n(r, z)$  and  $m$ . Consider case sounding of stratospheric aerosols at wavelengths 532 and 1064 nm as a first example. We obtained two-dimensional matrix  $c_{ij}$  of Eq.(5) for a situation, where two fractions of stratospheric aerosols were assumed. The designed procedure was used to process data on stratospheric sounding during the transformations of the stratospheric aerosol layer after the Pinatubo eruption. By our estimations, the error in Eq.(5) was 15 to 30% at different stages of the transformations. Thirdly, we use results of numerical experiments to estimate errors in Eq.(5).

### **Microphysical particle properties from 3-wavelength aerosol Raman lidar (UPIM and IfT):**

The performance characteristics of two algorithms, which were developed for these retrievals at the Institute of Mathematics of the University of Potsdam (IMP) and at the Institute for Tropospheric Research (IfT) were extensively studied (Böckmann, 2001 and Müller *et al.*, 1999).



Until now the studies focussed on the processing of the data sets from the 6-wavelength aerosol lidar of the IfT. The system provides profiles of the particle backscatter coefficients at 355, 400, 532, 710, 800, and 1064 nm, and of the particle extinction coefficients at 355 and 532 nm. Simulation studies are intended to show to which extent physical parameters can be retrieved from the reduced data set of 3 backscatter and 2 extinction coefficients. First results are given in Table 1.

Also shown are results for an experimental data set obtained with the 6-wavelength lidar during the Lindenberg Aerosol Characterization Experiment LACE 98 (Lindenberg/Germany, July/August 1998). A biomass-burning aerosol layer was observed in the free troposphere from 9-10 August 1998. The findings are presented in Wandinger *et al.* (2001). It can be shown that for this specific measurement case the particle backscatter spectrum can well be represented by the backscatter coefficients at 355, 532, and 1064 nm. Thus this measurement offered the opportunity to compare the results for the physical particle parameters from the inversion of the complete data set (6+2) and of the reduced data set (3+2). In addition airborne in-situ measurements during the lidar observations offered the unique possibility for a validation of the inversion results. With respect to the

$r_{\text{mod}}; \sigma$	0.1;1.4	0.1;1.6	0.1;1.8	0.3;1.6	LACE 98	LACE 98
$m_{\text{exact}}$	1.6+0.5i	1.5+0.01i	1.7+0.05i	1.4+0.005i	case 3+2	case 6+2
$r_{\text{eff}}$	0.13 (3.1;9.2)	0.17 (2.5;2.4)	0.24 (2.9;14.5)	0.51 (1.4;2.5)	$0.26 \pm 0.03$	$0.24 \pm 0.01$
$v_t$	0.007 (2;0.6)	0.011 (0.2;2.2)	0.02 (2;7.6)	0.304 (0.5;0.8)	$12 \pm 2$	$11 \pm 1$
$a_t$	0.158 (1.2;9.4)	0.195 (2.9;4.5)	0.251 (3.1;8.2)	1.758 (0.9;1.8)	$141 \pm 5$	$134 \pm 2$
$n_t$	1.0 (143;577)	1.0 (47;7.8)	1.0 (45;128)	1.0 (13;29)		$361 \pm 57$
$m_{\text{real}}$	$1.59 \pm 0.03$	$1.51 \pm 0.01$	$1.7 \pm 0.01$	$1.39 \pm 0.02$	$1.62 \pm 0.06$	$1.61 \pm 0.04$
$m_{\text{imag}}$	$0.51 \pm 0.02$	$0.012 \pm 0.003$	$0.057 \pm 0.005$	$0.005 \pm 0.0006$		$0.088 \pm 0.011$
$r_{\text{eff}}$	[0.15; 0.16±0.01]	[0.17; 0.16±0.1]	[0.25; 0.3±0.09]	[0.54; 0.61±0.13]	$0.27 \pm 0.04$	$0.27 \pm 0.04$
$v_t$	[0.0099; 0.0092±0.0008]	[0.012; 0.012±0.002]	[0.02; 0.027±0.009]	[0.31; 0.38±0.099]	$13 \pm 2$	$13 \pm 3$
$a_t$	[0.18; 0.17±0.01]	[0.21; 0.22±0.01]	[0.25; 0.26±0.01]	[1.74; 1.86±0.09]	$145 \pm 8$	$142 \pm 7$
$n_t$	[1.17; 1.09±0.095]	[1.15; 1.34±0.11]	[0.79; 0.66±0.28]	[0.84; 0.96±0.35]	$305 \pm 120$	$286 \pm 72$
$m_{\text{real}}$	$1.67 \pm 0.09$	$1.53 \pm 0.06$	$1.58 \pm 0.13$	$1.42 \pm 0.08$	$1.63 \pm 0.09$	$1.62 \pm 0.09$
$m_{\text{imag}}$	$0.4 \pm 0.08$	$0.015 \pm 0.0098$	$0.03 \pm 0.02$	$0.13 \pm 0.014$	$0.05 \pm 0.02$	$0.05 \pm 0.02$

$r_{\text{mod}}$  ( $\mu\text{m}$ )—mode radius,  $r_{\text{eff}}$  ( $\mu\text{m}$ )—effective radius,  $v_t$  ( $\mu\text{m}^3\text{cm}^{-3}$ )—total volume concentration,  $a_t$  ( $\mu\text{m}^2\text{cm}^{-3}$ )—total surface-area concentration,  $n_t$  ( $\text{cm}^{-3}$ )—total number concentration: exact value (error with known refractive index (%); error with unknown refractive index (%)), or [calculated value with known refractive index; calculated value with unknown refractive index], respectively,  $m_{\text{real}}$ —real part of refractive index,  $m_{\text{imag}}$ —imaginary part of refractive index.

Table 3.7: Results of the IMP (top) and IfT (bottom) algorithms: different simulations for the 3+2 case in the first four columns and physical particle parameters of lidar data for the height range from 3600–4100 m a.s.l. on 9 August 1998, 2200–2400 UTC in the last two columns.

experimental data excellent agreement of the results from the 3+2 with those from the 6+2 data set and also with the airborne in-situ measurements of particles with  $r \geq 50$  nm ( $r_{\text{eff}}=0.25 \pm 0.07$   $\mu\text{m}$ ,  $v_t=8 \pm 5$   $\mu\text{m}^3\text{cm}^{-3}$ ,  $a_t=95 \pm 55$   $\mu\text{m}^2\text{cm}^{-3}$ ,  $n_t=271 \pm 74$   $\text{cm}^{-3}$ ) was obtained. These results indicate that the 3+2 information is sufficient for a successful inversion in this case.

With respect to the IMP algorithm it was found that inversion errors increase with the reduction of measurement data and that a higher accuracy of the reduced data set is required for a successful inversion. Simulations showed that for noiseless data and known refractive index the mean and integral parameters of the particle size distribution, except the number concentration, which is always difficult to derive, can be limited to 3% error in the 6+2 case and to 5% error in the 3+2 case. For the unknown refractive index case this error increases to approximately 10%.

Böckmann, C. (2001). Hybrid regularization method for the ill-posed inversion of multiwavelength lidar data to retrieve aerosol size distribution. *Appl. Opt.*, **40**, pp. 1329-1342.

Müller, D., U. Wandinger and A. Ansmann. (1999). Microphysical particle parameters from extinction and backscatter lidar data by inversion with regularization: Theory. *Appl. Opt.*, **38**, 2346–2357.

Wandinger, U., D. Müller, C. Böckmann, D. Althausen, V. Matthias, J. Bösenberg, V. Weiß, M. Fiebig, M. Wendisch *et al.* (2001). Optical and microphysical characterization of biomass-burning and industrial-pollution aerosols from multiwavelength lidar and aircraft measurements. *J. Geophys. Res.* to appear.

**Investigations to the shape of the particles (UPIM):** The UPIM algorithm was extended to other shapes than spheres. We examined the influence of various spheroids with different aspect ratios on the retrieval process of the volumen distribution. The influence of spheroidal particles on the inversion process via spherical particles is not critical for monomodal distributions with small effective radii or for small spheroid's aspect ratios. In other cases we observed large differences, i.e. large errors. Therefore, depolarization measurements are necessary to classify the particles. On the other hand the hybrid regularization method of UPIM was improved to handle the spheroid's aspect ratio, if it is known, and presents excellent reconstruction results (Böckmann, Wauer 2000).

C. Böckmann, J. Wauer, The influence of spheroids on the inversion in the retrieval of microphysical particle parameters from lidar data , Proc. SPIE Intern. Soc. Opt. Eng. 4015, Sendai, Japan, October 2000.

### **3.17.4 Socio-Economic relevance and policy implication**

Microphysical properties of aerosols describe the particle's influence on the earth's radiation budget, on clouds and on precipitation, as well as their role in chemical processes of the troposphere and stratosphere. Warnings of climate change due to ozone depletion in the atmosphere have worried us for a number of years. One reason for the ozone depletion is the chlorine (Cl) in CFCs in the stratosphere. On the other side, polar stratospheric clouds (PSCs) are believed to play an active role in precursor stages of ozone depletion in the winter-cold stratosphere by catalyzing heterogeneous chemical reactions on their surface and by redistributing  $\text{HNO}_3$  through sedimentation. Knowledge about the aerosol surface area concentration is necessary to model processes involving ozone chemistry. The size distribution of these cloud particles is an important parameter for quantifying these mechanisms, because it relates the total surface to the total mass.

The investigations to the determination of microphysical parameters from a 3-wavelength aerosol Raman lidar (could be a standard lidar in future) are to our knowledge the first ones, therefore there will be significant interest in the science community to use these methods, for the improvement of global/regional atmospheric or of climate prediction models. Scientific publications and conference presentations, resulting from WP17, will give the opportunity to the science community to address the mechanisms of local aerosol formation, to study the trans-boundary transport processes of air pollution over Europe and to study the impact of aerosol loads in the earth's radiation budget and their link to Global Change. Finally, the investigations could be proposed for an air pollution abatement strategy in Europe, in compliance with the EU air pollution abatement/Climate Change policy.

### **3.17.5 Discussion and conclusion**

In general, it was found that inversion errors increase with the reduction of measurement data and that a higher accuracy of the reduced data set is required for a successful inversion. Simulations with the UPIM algorithm showed that for noiseless data and known refractive index the mean and integral parameters of the particle size distribution, except the number concentration, can be limited to 3% error in the 6+2 case. For the reduced data set this error increases to 5%. Errors in the input

data of the order of 10% lead to errors in the physical particle parameters of 7% for the 6+2 case and of approximately estimated to 15% in the 3+2 case.

### **3.17.6 Plan and Objectives for the next period**

Important activities, in full accordance with the contract, were implemented right from the start of the project.

For the next period the groups UPIM and IfT will continue the investigations with respect to a minimum data set. This is planned especially by examinations with different noisy data. Further investigations are necessary concerning the determination of the imaginary part of the refractive index which is very sensitive in the inversion process.

Secondly, the completion of the development of the 1-dimensional inversion algorithm with a user-friendly editing (UPIM) of the software is planned.

Thirdly, further investigations will be done in the next time to continue the influence of spheroids and additionally to examine the influence of inhomogeneous particles on the inversion process.

Finally, during the next period, the IPNANB group assume to compute the matrix of coefficients  $c_{ij}$  for two- to four-frequency sounding of rural aerosols and to study opportunities of estimating moments  $\langle r^2 \rangle$  and  $\langle r^3 \rangle$ . In addition, they will design an algorithm to compute the matrix  $c_{ij}$  with taking possible additional information from independent measurements into account and believe to implement this procedure by introducing additional terms in functional (6). First of all, they will investigate opportunities provided by observing spectral atmospheric attenuation with the aid of a Sun photometer. Results of these measurements will be available for them from observations at Belsk and Minsk in the nearest future.

## **3.18 General project assessment**

### **3.18.1 Objectives**

The objectives of the project in the reporting period were

1. to bring the lidar systems at all stations to a status that reliable, quantitative measurements on a regular schedule are possible,
2. to establish common retrieval procedures,
3. to perform regular measurements,
4. to establish a common data base for the measurements and the associated trajectories,
5. to perform comprehensive measures for quality assurance, for both instruments and retrieval algorithms,
6. to establish the necessary organisation for the performance of special measurements.

### **3.18.2 Scientific achievements**

All of the objectives for this period have been achieved to a very large extent. The main result is the most comprehensive and systematically collected data base of the aerosol vertical distribution on a continental scale that is presently available. This data base is now steadily growing during the course of the project. A very important subset of the data contains material for studies of medium to long range transport of Saharan dust to Europe in general and the Mediterranean in particular. The development of the methodology for analysis of the data, both with respect to microphysical properties and for statistical studies has also made good progress.

### **3.18.3 Socio-economic relevance and policy implications**

As a first result the formation and operation of a real network on the European scale, including 20 groups from 11 countries, is a major step forward towards a truly cooperative scientific community in the area of advanced remote sensing and experimental environmental studies. It is anticipated that this cooperation will be extended to the joint analysis of data, addressing issues that are relevant on a European rather than on a national scale.

The data base that has been established and that is now growing continuously is of very high scientific interest, because it is by far the most comprehensive quantitative data set on the vertical distribution of aerosols on a continental scale. With growing statistical significance it will become an excellent tool for checking and improving models that explain and predict the aerosol load and its effects on the radiation budget, the water cycle, and human life.

### **3.18.4 Plan for the next period**

The most important task for the next period is to continue the regular measurements as scheduled to increase the statistical significance of the data set. In addition a number of special measurements for various studies of aerosol-related problems is planned.

Data analysis will be devoted to special case studies, but also the statistical analysis has to be started, including the development of appropriate tools. Considering the progress made up to now it appears likely that the goals can be reached.

# Bibliography

- [Böckmann and Wauer, 2000] Böckmann, C. and Wauer, J. (2000). The influence of spheroids on the inversion in the retrieval of microphysical particle parameters from lidar data. In *Proc. SPIE Intern. Soc. Opt. Eng. 4015, Sendai, Japan*.
- [Bösenberg, 2001] Bösenberg, J. (2001). The german aerosol lidar network: Methodology, data, analysis. MPI-Report, Max-Planck-Institut für Meteorologie, Hamburg.
- [Bösenberg et al., 2000] Bösenberg, J., Ansmann, A., Baldasano, J., Balis, D., Böckmann, C., Calpini, B., Chaikovsky, A., Flamant, P., Hagard, A., Mitev, V., Papayannis, A., Pelon, J., Resendes, D., Schneider, J., Spinelli, N., Vaughan, T. T. G., Visconti, G., and Wiegner, M. (2000). EARLINET: A European Aerosol Research Lidar Network. In Dabas, A. and Pelon, J., editors, *Laser Remote Sensing of the Atmosphere. Selected Papers of the 20<sup>th</sup> International Laser Radar Conference*. Edition Ecole Polytechnique, Palaiseau, in press.
- [Dorling et al., 1992] Dorling, S., Davies, T., and Pierce, C. (1992). Cluster analysis: A technique for estimating the synoptic meteorological controls on air and precipitation chemistry-method and applications. *Atmos. Environ.*, 26A:2575–2581.
- [Kottmeier and Fay, 1998] Kottmeier, C. and Fay, B. (1998). Trajectories in the antarctic lower troposphere. *JGR*, 103(D9):10947–10959.
- [Mattis et al., 2001] Mattis, I., Jaenisch, V., Müller, D., Franke, K., , and Ansmann, A. (2001). Classification of particle extinction profiles derived within the framework of the german lidar network by the use of cluster analysis of backtrajectories. In Dabas, A. and Pelon, J., editors, *Laser remote sensing of the atmosphere. Selected papers of the 20th International Laser Radar Conference*. Ecole Polytechnique.
- [Schneider et al., 2000] Schneider, J., Ansmann, A., Baldasano, J., Balis, D., Böckmann, C., Bösenberg, J., Calpini, B., Chaikovsky, A., Flamant, P., Hagard, A., Mitev, V., Papayannis, A., Pelon, J., Resendes, D., Spinelli, N., Vaughan, T. T. G., Visconti, G., and Wiegner, M. (2000). A European Aerosol Research Lidar Network to Establish an Aerosol Climatology: EARLINET. *J. Aerosol Science*, 31:592–593.
- [Stohl, 1998] Stohl, A. (1998). Computation, accuracy and applications of trajectories —a review and bibliography. *Atmos. Environ.*, 32(6):947–966.